

# Synthesis and Pharmacological Characterization of N<sup>3</sup>-Substituted Willardiine Derivatives: Role of the Substituent at the 5-Position of the Uracil Ring in the Development of Highly Potent and Selective GLU<sub>K5</sub> Kainate Receptor Antagonists

Nigel P. Dolman,<sup>†</sup> Julia C. A. More,<sup>†</sup> Andrew Alt,<sup>§</sup> Jody L. Knauss,<sup>§</sup> Olli T. Pentikäinen,<sup>†</sup> Carla R. Glasser,<sup>||</sup> David Bleakman,<sup>§</sup> Mark L. Mayer,<sup>||</sup> Graham L. Collingridge,<sup>‡</sup> and David E. Jane<sup>\*,†</sup>

Department of Pharmacology, MRC Centre for Synaptic Plasticity, School of Medical Sciences, University Walk, University of Bristol, Bristol BS8 1TD, United Kingdom, Department of Anatomy, MRC Centre for Synaptic Plasticity, School of Medical Sciences, University of Bristol BS8 1TD, United Kingdom, Neuroscience Research, Eli Lilly and Company, Lilly Corporate Center, Indianapolis, Indiana 46285, and Laboratory of Cellular and Molecular Neurophysiology, Porter Neuroscience Research Center, National Institute of Child Health and Human Development, National Institutes of Health, Department of Health and Human Services, Bethesda, Maryland 20892

Received August 30, 2006

Some N<sup>3</sup>-substituted analogues of willardiine such as **11** and **13** are selective kainate receptor antagonists. In an attempt to improve the potency and selectivity for kainate receptors, a range of analogues of **11** and **13** were synthesized with 5-substituents on the uracil ring. An X-ray crystal structure of the 5-methyl analogue of **13** bound to GLU<sub>K5</sub> revealed that there was allowed volume around the 4- and 5-positions of the thiophene ring, and therefore the 4,5-dibromo and 5-phenyl (**67**) analogues were synthesized. Compound **67** (ACET) demonstrated low nanomolar antagonist potency on native and recombinant GLU<sub>K5</sub>-containing kainate receptors ( $K_B$  values of  $7 \pm 1$  and  $5 \pm 1$  nM for antagonism of recombinant human GLU<sub>K5</sub> and GLU<sub>K5</sub>/GLU<sub>K2</sub>, respectively) but displayed  $IC_{50}$  values  $> 100 \mu M$  for antagonism of GLU<sub>A2</sub>, GLU<sub>K6</sub>, or GLU<sub>K6</sub>/GLU<sub>K2</sub>.

## Introduction

Kainate receptors are a class of ligand-gated ion channel that are expressed in the mammalian central nervous system and are activated by the excitatory neurotransmitter (*S*)-glutamate.<sup>1</sup> There are three groups of ligand-gated ion channels activated by (*S*)-glutamate known as the (*S*)-2-amino-3-hydroxy-5-methyl-4-isoxazolepropanoic acid (AMPA,<sup>a</sup> **1**, Figure 1), (2*S*,3*S*,4*S*)-3-carboxymethyl-4-isopropenyl-pyrrolidine-2-carboxylic acid (kainate, **2**), and *N*-methyl-D-aspartic acid (NMDA) receptor subtypes.<sup>2</sup> Kainate receptors are tetrameric assemblies of GLU<sub>K5-7</sub>, GLU<sub>K1</sub>, and GLU<sub>K2</sub> subunits (IUPHAR nomenclature of the receptors that are also known as GluR5–7, KA1, and KA2).<sup>3</sup> AMPA receptors are tetrameric assemblies of a combination of GLU<sub>A1-4</sub> subunits (IUPHAR nomenclature of the receptors that are also known as GluR1–4 or GluRA–D).<sup>3</sup> The first antagonists with significant activity at kainate receptors were from the quinoxalinedione class of compounds, and these included 6-cyano-7-nitroquinoxaline-2,3-dione (CNQX, **3**) and the potent AMPA receptor antagonist 2,3-dihydroxy-6-nitro-7-sulfamoyl-benzo(*f*)quinoxaline (NBQX, **4**).<sup>4</sup> None of these compounds were useful as pharmacological tools for kainate receptors as they also antagonized AMPA receptors. More recently, a series of decahydroisoquinolines, culminating in compound **5**,<sup>5f</sup> have been reported as selective GLU<sub>K5</sub>-contain-

ing kainate receptor antagonists.<sup>5,6</sup> These antagonists displayed useful selectivity for GLU<sub>K5</sub> versus AMPA and GLU<sub>K6</sub>-containing receptors and were therefore used to provide evidence to support the role of GLU<sub>K5</sub> in synaptic plasticity in the mossy fiber to CA3 region of the hippocampus and in a number of central nervous system disorders such as chronic pain, epilepsy, ischaemia, and migraine.<sup>5,6</sup> Interestingly, an analogue of the natural product dysiherbaine, **6**, has been reported to be a selective GLU<sub>K5</sub> receptor antagonist.<sup>7</sup> However, unlike the decahydroisoquinoline-based antagonists, **6** evoked brief seizures followed by unconsciousness when injected into mice.<sup>8</sup> Aside from orthosteric antagonists, recently the first selective non-competitive antagonist for GLU<sub>K5</sub>, **7**, has been reported.<sup>9</sup>

Substitution at the 5-position of the uracil ring of the natural product willardiine (**8**) led to compounds (**9** and **10**) with selective agonist activity at either AMPA or kainate receptors.<sup>10</sup> We have produced selective GLU<sub>K5</sub>-containing kainate receptor antagonists by adding either a 2-carboxybenzyl (**11**) or a 2-carboxythiophene-3-ylmethyl (**13**) substituent to the N<sup>3</sup>-position of the uracil ring of willardiine.<sup>11</sup> The racemic mixture and the pure *S* enantiomer **11** have been used to show that the kainate receptor involved in the induction of long-term potentiation (LTP) in the mossy fiber to CA3 pathway in the hippocampus contains the GLU<sub>K5</sub> subunit.<sup>11,12</sup> In addition, **11** has been used to show that GLU<sub>K5</sub>-containing kainate receptors are involved in short-term recognition memory.<sup>13</sup> We have reported previously that **12**, the 5-iodo-substituted analogue of **11**, had enhanced GLU<sub>K5</sub> antagonist potency and selectivity, but replacement of the thiophene ring of **13** with a furan ring to give **14** led to a reduction in GLU<sub>K5</sub> receptor antagonist potency.<sup>11</sup>

While **11**–**14** (Figure 1) were moderately potent kainate receptor antagonists, there is a need for more potent and selective antagonists for *in vitro* and *in vivo* studies of GLU<sub>K5</sub> kainate receptor function. Herein, we report the synthesis and pharmacological characterization of a new series of analogues of **11** and **14** in which the 5-substituent on the uracil ring was varied

\* To whom correspondence should be addressed. Phone: +44 (0)117 9546451. Fax: +44 (0)117 9250168. E-mail: david.jane@bristol.ac.uk.

<sup>†</sup> Department of Pharmacology, University of Bristol.

<sup>‡</sup> Department of Anatomy, University of Bristol.

<sup>§</sup> Eli Lilly and Co.

<sup>||</sup> NIH.

<sup>a</sup> Abbreviations: AMPA, (*S*)-2-amino-3-hydroxy-5-methyl-4-isoxazolepropanoic acid; kainate, (2*S*,3*S*,4*S*)-3-carboxymethyl-4-isopropenyl-pyrrolidine-2-carboxylic acid; NMDA, *N*-methyl-D-aspartic acid; CNQX, 6-cyano-7-nitroquinoxaline-2,3-dione; NBQX, 2,3-dihydroxy-6-nitro-7-sulfamoyl-benzo(*f*)quinoxaline; DHPG, (*S*)-3,5-dihydroxyphenylglycine; fDR-VRP, fast component of the dorsal root-evoked ventral root potential; ATPO, (*S*)-2-amino-3-[5-*tert*-butyl-3-(phosphonomethoxy)-4-isoxazolyl]propionic acid.

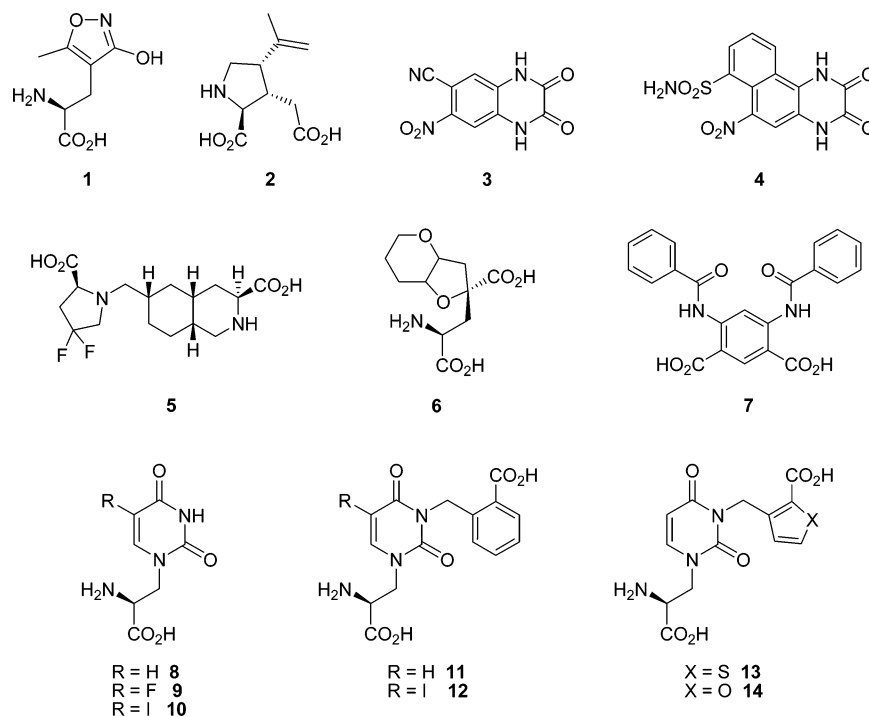


**Figure 1.** Structures of AMPA and kainate receptor agonists and antagonists.

in an attempt to increase the potency and selectivity for GLU<sub>K5</sub>-containing kainate receptors. In addition, the effect of adding substituents to the thiophene ring was investigated. This novel series of compounds was pharmacologically characterized on both cloned and native AMPA and kainate receptors. We also undertook a molecular modeling study to attempt to explain the pharmacological data obtained for the compounds synthesized in this study.

## Results

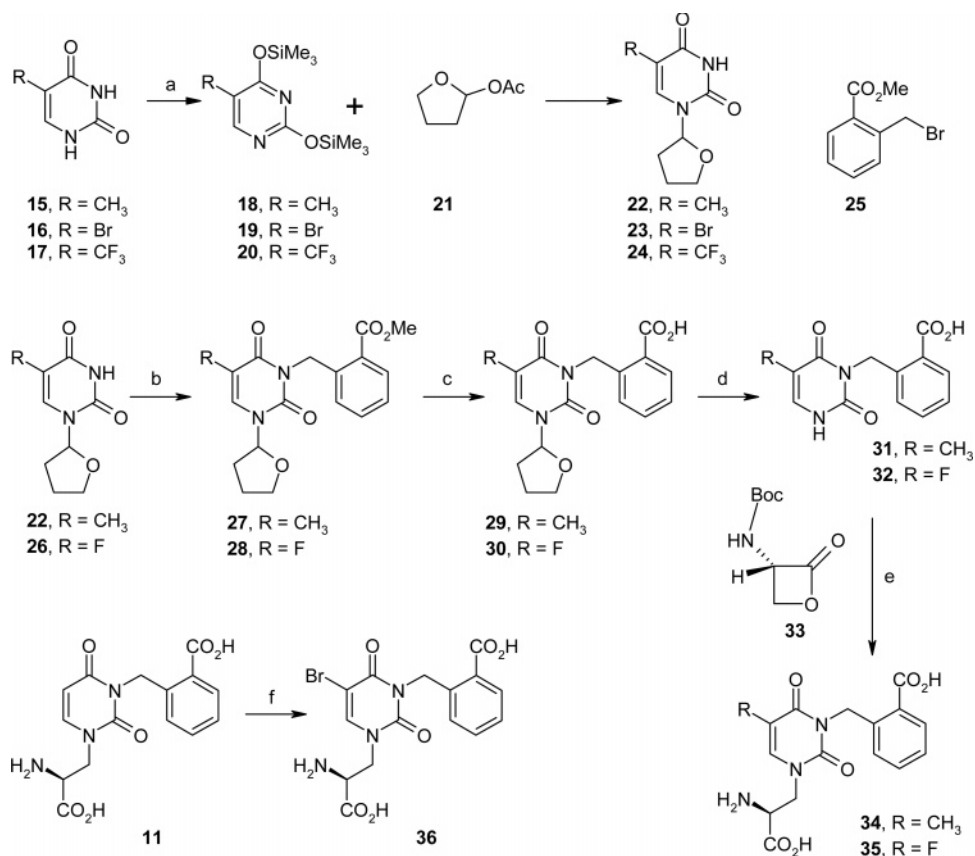
**Chemistry.** A series of 5-substituted analogues of the previously reported GLU<sub>K5</sub> selective antagonist **11** were synthesized, as we had previously observed that **12**, the 5-iodo-substituted analogue of **11** (Figure 1), had increased GLU<sub>K5</sub> antagonist potency and selectivity.<sup>11a</sup>

The required 5-substituted N<sup>1</sup>-protected uracil **22**<sup>14</sup> was synthesized from thymine (**15**). Heating a suspension of thymine (**15**) in the presence of hexamethyldisilazane, TMSCl, and ammonium sulfate catalyst until a clear solution resulted produced the silylated uracil (**18**) (Scheme 1).<sup>15</sup> The highly moisture-sensitive silylated uracil (**18**) was then treated with a large excess of 2-acetoxytetrahydrofuran (**21**), prepared by a previously reported route.<sup>11b</sup> Treatment of the resulting mixture of N<sup>1</sup>- and N<sup>1</sup>,N<sup>3</sup>-di-substituted products with ethanol/acetic acid<sup>16</sup> resulted in total hydrolysis back to the free uracil (**15**). Therefore, the quantity of 2-acetoxytetrahydrofuran (**21**) was reduced to only a slight excess to minimize the formation of the N<sup>1</sup>,N<sup>3</sup>-di-substituted product. Alkylation of **22** with the substituted benzyl bromide **25**<sup>17</sup> gave the N<sup>3</sup>-substituted uracil **27**. Similarly, alkylation of commercially available fluorouracil (**26**) with the substituted benzyl bromide (**25**) gave the corresponding 5-fluoro-substituted derivative **28**. Subsequent basic hydrolysis of the methyl esters (**27** and **28**) afforded the free carboxylic acids (**29** and **30**), which give the N<sup>3</sup>-substituted uracil derivatives (**31** and **32**) following treatment with TFA to remove the N<sup>1</sup> protecting group. Treatment of the sodium salts of **31** and **32** with (*S*)-*N*-Boc-serine-β-lactone (**33**)<sup>18</sup> in DMF, followed by hydrolysis of the N-Boc-protected intermediates with 2 M

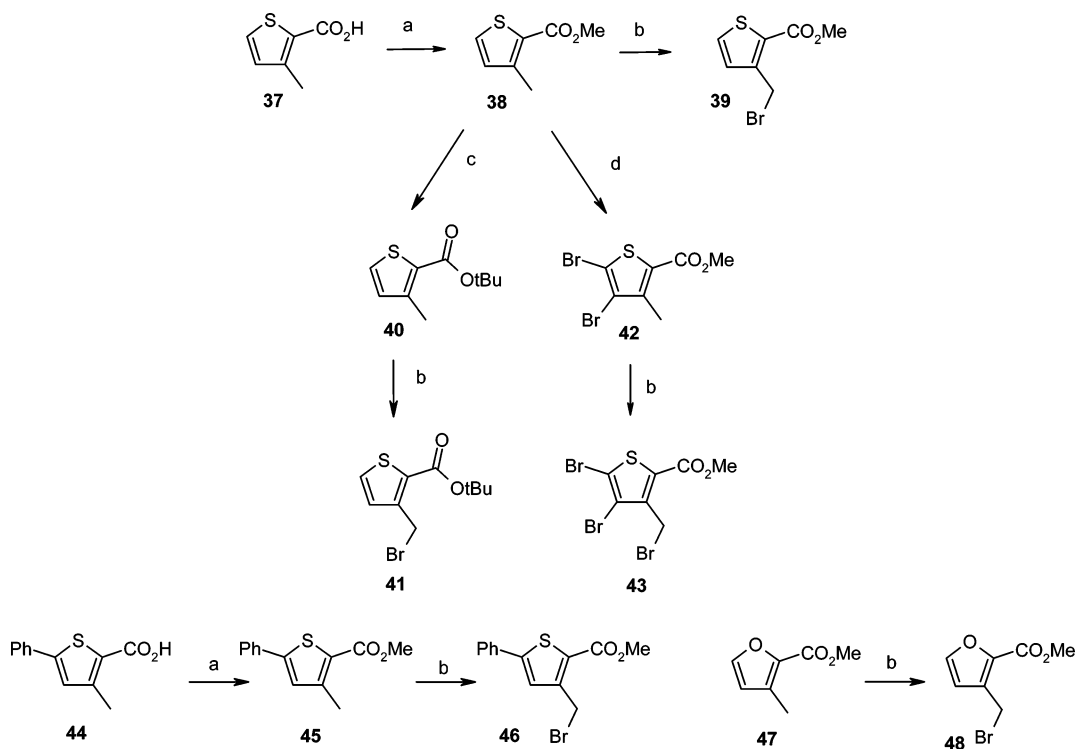
HCl (aq), gave amino acids **34** and **35** with enantiomeric excesses >99% as determined by chiral HPLC. Compound **11**<sup>11a</sup> was treated with bromine in aqueous acetic acid to obtain the 5-bromo derivative (**36**, Scheme 1), which was purified using Dowex 50WX8 ion-exchange resin (H<sup>+</sup> form) and crystallization from water, thereby avoiding the use of strongly basic Dowex X18 resin.

The N<sup>1</sup>-protected uracils **22**, **23**, and **24** were required for the synthesis of a range of 5-substituted analogues of the sub-micromolar potent GLU<sub>K5</sub> antagonist **13**. The 5-trifluoromethyl derivative (**24**) was synthesized from the corresponding uracil (**17**) by the method used for the preparation of **22**. In the case of the 5-bromo derivative **23**,<sup>14</sup> the protected uracil (**19**) was treated with an excess of 2-acetoxytetrahydrofuran (**21**), and the resulting N<sup>1</sup>- and N<sup>1</sup>,N<sup>3</sup>-di-protected products were then hydrolyzed with a mixture of ethanol/acetic acid<sup>11b,16</sup> to give almost exclusively the N<sup>1</sup>-protected uracil derivative (**23**) (see Scheme 1).

The thiophene ester (**39**)<sup>11b,19</sup> required for the synthesis of the N<sup>3</sup>-substituted derivatives **52**–**54** was synthesized by esterification of the carboxylic acid (**37**) followed by treatment of the ester (**38**) with NBS under free radical conditions (Scheme 2). The initial attempt at the synthesis of the N<sup>3</sup>-substituted uracil (**54**) involved the treatment of the sodium salt of **24** with thiophene ester (**39**). However, attempted conversion of the methyl ester to the corresponding carboxylic acid via base hydrolysis of the N<sup>3</sup>-substituted intermediate led to hydrolysis of the 5-trifluoromethyl group to a carboxylic acid. To circumvent this problem, the commercially available methyl ester (**38**) was treated with an excess of potassium *t*-butoxide in diethyl ether to afford the *t*-butyl ester (**40**). Treatment of **40** with NBS under free radical conditions gave the bromomethyl derivative (**41**), and this ester was used for the preparation of the N<sup>3</sup>-substituted derivatives **52**–**54** (Scheme 2). Reaction of the sodium salt of **24** with the *t*-butyl ester (**40**) gave the N<sup>3</sup>-substituted intermediate (**51**) (Scheme 3). Concomitant deprotection of the *t*-butyl ester and the N<sup>1</sup>-protecting group of **51** was achieved by treatment with TFA to afford the N<sup>3</sup>-substituted

Scheme 1<sup>a</sup>

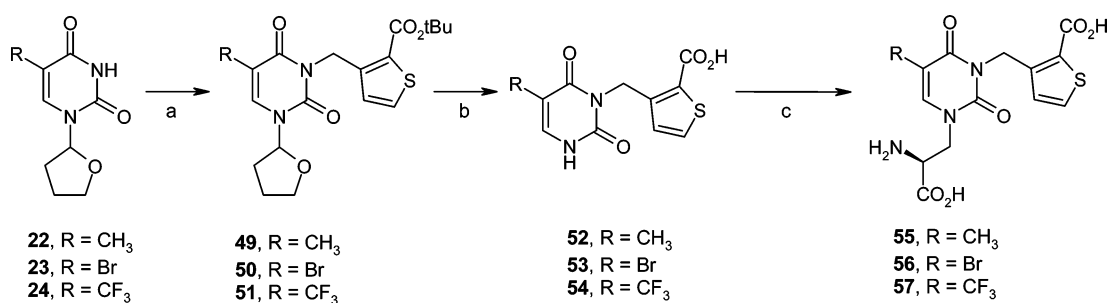
<sup>a</sup> (a) (i) HMDS, TMSCl, (NH<sub>4</sub>)<sub>2</sub>SO<sub>4</sub>, reflux; (b) (i) NaH, DMF, (ii) **25**; (c) LiOH, dioxane/water (1:1), room temperature; (d) TFA, room temperature; (e) (i) 2 equiv of NaH, DMF, room temperature, (ii) **33**, (iii) 2 M HCl, 50 °C; (f) Br<sub>2</sub>/AcOH (aq).

Scheme 2<sup>a</sup>

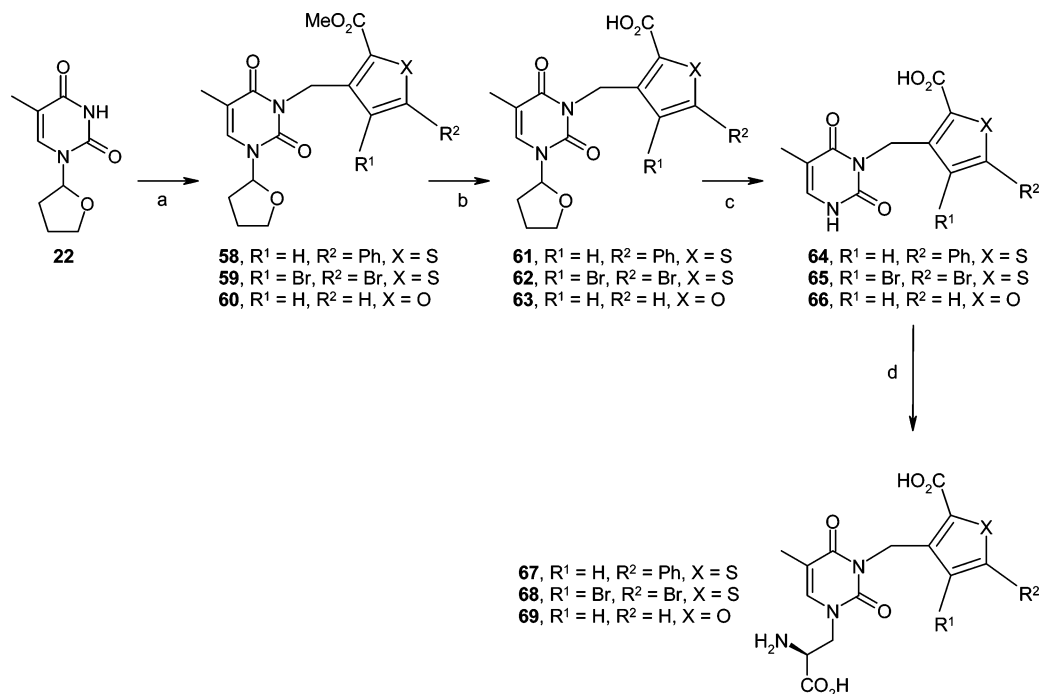
<sup>a</sup> (a) MeOH, H<sub>2</sub>SO<sub>4</sub>, reflux; (b) NBS, benzoyl peroxide, CCl<sub>4</sub>; (c) KO<sup>t</sup>Bu, Et<sub>2</sub>O; (d) Br<sub>2</sub>, AcOH, room temperature.

uracil (**54**). Similarly, the N<sup>3</sup>-substituted uracils **52** and **53** were synthesized by alkylation of the corresponding N<sup>1</sup>-protected uracils **22** and **23** with *t*-butyl ester (**40**), followed by treatment

with TFA (Scheme 3). The amino acids **55**–**57** were synthesized by treatment of the sodium salts of the corresponding uracils (**52**–**54**) with (*S*)-*N*-Boc-serine-β-lactone (**33**) in DMF, followed

Scheme 3<sup>a</sup>

<sup>a</sup> (a) (i) NaH, DMF, room temperature, (ii) **41** (Scheme 2), DMF, room temperature; (b) TFA, room temperature; (c) (i) 2 equiv of NaH, DMF, room temperature, (ii) **33** (Scheme 1), (iii) 2 M HCl, 50 °C.

Scheme 4<sup>a</sup>

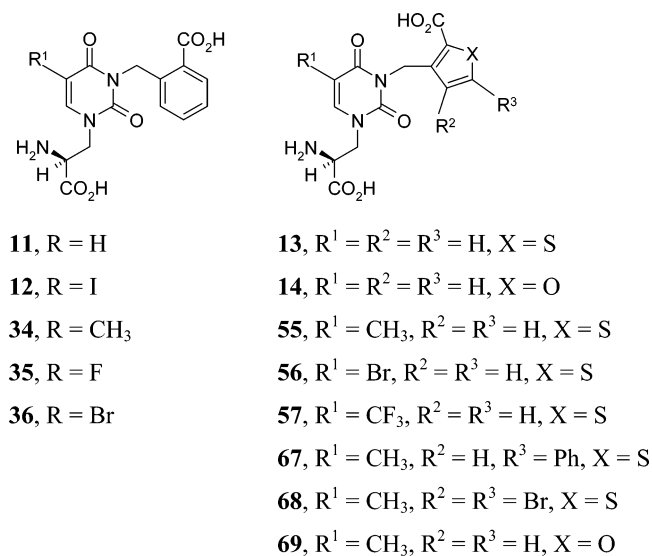
<sup>a</sup> (a) (i) NaH, DMF, (ii) **43**, **46**, or **48** (Scheme 3), 60 °C; (b) LiOH, dioxane/water (1:1); (c) TFA, room temperature; (d) (i) 2 equiv of NaH, DMF, room temperature, (ii) **33** (Scheme 1), (iii) 2 M HCl, 50 °C.

by removal of the Boc protecting group with 2 M HCl (aq) and purification by ion-exchange chromatography and crystallization from water (Scheme 3).

An analogue of **55** in which the thiophene ring is replaced with a furan ring (**69**) was synthesized by reacting the bromomethylfuran (**48**) with the sodium salt of the N<sup>1</sup>-protected uracil (**22**) to give the N<sup>3</sup>-substituted intermediate (**60**) (Scheme 4). The bromomethylfuran (**48**)<sup>20</sup> was synthesized from commercially available furan **47** (Scheme 2) by treatment with NBS under free radical conditions. The ester (**60**) was hydrolyzed with aqueous lithium hydroxide to give **63**, which was treated with TFA to give the N<sup>3</sup>-substituted uracil (**66**). The amino acid (**69**) was obtained by reacting the sodium salt of **66** with (*S*)-*N*-Boc-serine- $\beta$ -lactone (**33**) and removal of the Boc group of the resulting intermediate with TFA (Scheme 4). The phenyl-substituted thiophene (**46**) was synthesized starting from **44**<sup>22</sup> (Scheme 2), which was prepared by a previously reported method. Esterification of **44** with methanol/H<sub>2</sub>SO<sub>4</sub> and treatment of the resultant ester (**45**) with NBS gave the required bromomethylthiophene (**46**) (Scheme 2). Alkylation of the sodium salt of **22** with **46** afforded the N<sup>3</sup>-substituted intermediate, which was hydrolyzed with LiOH, and the N<sup>1</sup> protecting group was removed with TFA to give the desired uracil (**64**) (Scheme 4).

The amino acid (**67**) was obtained from **64** by the same method employed for the synthesis of **69** (Scheme 4). The known dibromothiophene (**42**)<sup>23</sup> was obtained by treatment of the ester (**38**) with excess bromine in acetic acid (Scheme 2). Bromination of **42** with NBS under free radical conditions gave the bromomethyl derivative (**43**), which was used to alkylate the sodium salt of **22**. The resultant N<sup>3</sup>-substituted intermediate (**59**) was converted to the amino acid (**68**) using methods similar to those used for the synthesis of **67** and **69** (Scheme 4).

**Pharmacology. In Vitro Electrophysiology. Native GLU<sub>K5</sub> Kainate Receptor Antagonist Activity.** Neonatal rat dorsal root C fibers are a convenient source of GLU<sub>K5</sub>-containing kainate receptors<sup>24</sup> for the assessment of the antagonist activity of N<sup>3</sup>-substituted willardiines.<sup>11</sup> In this assay, the known AMPA/kainate receptor antagonist **3** (Figure 1) had low micromolar potency as an antagonist of kainate-induced depolarizations (see Table 1 for data), which is in agreement with a previous report.<sup>25</sup> We have shown previously that **11** and **13** are selective sub-micromolar potent GLU<sub>K5</sub> receptor antagonists in this assay.<sup>11</sup> Adding a substituent to the 5-position of the uracil ring of **11** improved GLU<sub>K5</sub> receptor antagonist potency and selectivity versus AMPA receptors. The rank order of antagonist potency for the 5-substituted analogues of **11** was 5-CH<sub>3</sub> > 5-Br > 5-I

**Table 1.** Summary of the Activity of Novel N<sup>3</sup>-Substituted Willardiine Analogues at AMPA and Kainate Receptors in Electrophysiological Assays<sup>a</sup>

compound	K <sub>D</sub> (μM) vs kainate <sup>b</sup>	IC <sub>50</sub> (μM) vs fDR-VRP <sup>c</sup>
<b>3</b>	1.38 ± 0.12	
<b>4</b>		0.214 ± 0.043
<b>11</b>	0.402 ± 0.045 <sup>d</sup>	106 ± 13 <sup>d</sup>
<b>12</b>	0.209 ± 0.019 <sup>d</sup>	74.1 ± 4.3 <sup>d</sup>
<b>13</b>	0.105 ± 0.007 <sup>d</sup>	31.2 ± 5.0 <sup>d</sup>
<b>14</b>	1.88 ± 0.15 <sup>d</sup>	11.7 ± 1.3 <sup>d</sup>
<b>34</b>	0.023 ± 0.001	51.2 ± 8.6
<b>35</b>	0.358 ± 0.013	18.5 ± 4.4
<b>36</b>	0.102 ± 0.020	63.9 ± 16.2
<b>55</b>	0.018 ± 0.004	16.2 ± 5.4
<b>56</b>	0.025 ± 0.002	42.9 ± 8.2
<b>57</b>	0.055 ± 0.010	55.3 ± 9.6
<b>67</b>	0.012 ± 0.001	16.6 ± 1.1
<b>68</b>	0.010 ± 0.002	2.8 ± 0.8
<b>69</b>	0.080 ± 0.008	25.1 ± 3.7

<sup>a</sup> All values are from three independent experiments and are expressed as the mean ± SEM. <sup>b</sup> Apparent K<sub>D</sub> values for antagonism of kainate-induced depolarization of neonatal rat dorsal root fibers calculated using the Gaddum–Schild equation. <sup>c</sup> Depression of the fast component of the dorsal root evoked ventral root potential (fDR-VRP) in the neonatal rat spinal cord preparation, a measure of antagonist activity at AMPA receptors expressed on motoneurons. <sup>d</sup> Values taken from refs 11a,b. <sup>e</sup> K<sub>D</sub> values for inhibition by **13**, **55**, and **67** of the depolarization of neonatal rat motoneurons induced by **9** (a selective AMPA receptor agonist) were 71.4 ± 8.3, 83.4 ± 4.1, and 108 ± 6 μM (*n* = 3; mean ± SEM), respectively.

> 5-F ≈ 5-H. A series of 5-substituted analogues of **13** was synthesized, and again the 5-methyl-substituted analogue (**55**) gave the most potent GLU<sub>K5</sub> receptor antagonist (see Figure 2A for a concentration–response curve for kainate-induced depolarization of dorsal root C fibers in the absence and presence of **55**) with the rank order of potency being 5-CH<sub>3</sub> > 5-Br > 5-CF<sub>3</sub>. We have previously reported that **14**, the analogue of **13** with a furan rather than a thiophene ring, was 18-fold less potent as a GLU<sub>K5</sub> receptor antagonist.<sup>11b</sup> However, the 5-methyl analogue **69** was >20-fold more potent than the parent compound **14**, but **69** was still 4-fold less potent than the corresponding thiophene ring-containing compound **55**. Adding substituents to the thiophene ring of **55** improved potency as both **67** and **68** proved to be highly potent antagonists of native GLU<sub>K5</sub> receptors.

**Native AMPA Receptor Antagonist Activity.** The ability of compounds to reduce the fast component of the dorsal root-evoked ventral root potential (fDR-VRP), which is mediated

by AMPA receptors expressed on neonatal rat motoneurons,<sup>26</sup> was used as an expeditious method of investigating the relative antagonist potency at AMPA receptors (see Table 1 for data). All of the compounds tested were greater than 13-fold less potent as AMPA receptor antagonists than the reference substance **4** (Figure 1). For the most potent GLU<sub>K5</sub> kainate receptor antagonists, apparent K<sub>D</sub> values for the antagonism of depolarizations of neonatal rat motoneurons induced by **9** (a selective AMPA receptor agonist) were calculated. Apparent K<sub>D</sub> values for antagonism of depolarizations induced by **9** for compounds **13**, **55**, and **67** were 71.4 ± 8.3, 83.4 ± 4.1, and 108 ± 6 μM, respectively. Figure 2B illustrates a concentration–response curve for (*S*)-5-fluorowillardiine (**9**)-induced depolarization of neonatal rat motoneurons in the absence and presence of **55**.

**Antagonist Activity on NMDA and Group I Metabotropic Glutamate Receptors Expressed on Neonatal Rat Motoneurons.** Two of the most potent and selective GLU<sub>K5</sub> receptor antagonists **55** and **67** were tested on NMDA and group I (mGlu1 and mGlu5) metabotropic glutamate receptors expressed on neonatal rat motoneurons. Compounds **55** (10 μM) and **67** (1 μM) had no activity on NMDA- or (*S*)-3,5-dihydroxyphenylglycine (DHPG, a mGlu1 and mGlu5 receptor agonist)-induced depolarizations of neonatal rat motoneurons (*n* = 3).

**Calcium Fluorescence Assays. Recombinant Human AMPA and Kainate Receptor Subtypes.** To further characterize the selectivity of **55** and **67**, two of the most potent and selective GLU<sub>K5</sub> receptor antagonists identified in the native ionotropic glutamate receptor assays, they were tested on a range of recombinant human AMPA and kainate receptor subtypes (see Table 2 for data). Compounds **55** and **67** were highly potent antagonists of cells expressing GLU<sub>K5</sub> with K<sub>b</sub> values of 10 ± 1 and 7 ± 1 nM, respectively. Similar potencies were observed upon testing **55** and **67** on GLU<sub>K5</sub>/GLU<sub>K2</sub> heteromers where K<sub>b</sub> values of 8 ± 2 and 5 ± 1 nM, respectively, were obtained. Neither of these compounds had significant activity at GLU<sub>A2</sub>, GLU<sub>K6</sub>, or GLU<sub>K6</sub>/GLU<sub>K2</sub> receptors (IC<sub>50</sub> values >100 μM). Figure 2C illustrates concentration response curves for antagonism of glutamate-induced Ca<sup>2+</sup> fluorescence by **55** in cell lines expressing human GLU<sub>K5</sub>, GLU<sub>K5</sub>/GLU<sub>K2</sub>, or GLU<sub>K6</sub>.

**Modeling Study.** To understand the pharmacological data obtained for the new compounds, we undertook a molecular modeling study in which the recently reported X-ray crystal structures of **11** and **55** bound to the ligand binding core of GLU<sub>K5</sub><sup>21</sup> were used as a template. To investigate the reasons for the low affinity of **67** for AMPA receptors, attempts were made to dock it into the ligand binding core of GLU<sub>A2</sub>.

**Protein Structures.** The crystal structure of the ligand binding domain of GLU<sub>A2</sub> in complex with bound antagonist ligand (*S*)-2-amino-3-[5-*tert*-butyl-3-(phosphonomethoxy)-4-isoxazolyl]propionic acid (ATPO) (PDB code: 1NOT)<sup>27</sup> and the GLU<sub>K5</sub> ligand binding core in complex with the antagonist ligands **55** (PDB code: 2F34)<sup>21</sup> and **11** (PDB code: 2F35)<sup>21</sup> were used in this study. Hydrogen atoms for all protein structures and models were added using the program Reduce.<sup>28</sup> The flexibility of amino acid side chains was modeled by using the amino acid side-chain rotamer library<sup>29</sup> incorporated within the BODIL<sup>30</sup> modeling environment.

**Ligand Structures.** Ligand structures were optimized quantum mechanically (QM) with Gaussian 03<sup>31</sup> at the B3LYP/6-31+G\* level using a continuum solvent model (water, using the PCM model of Gaussian 03).

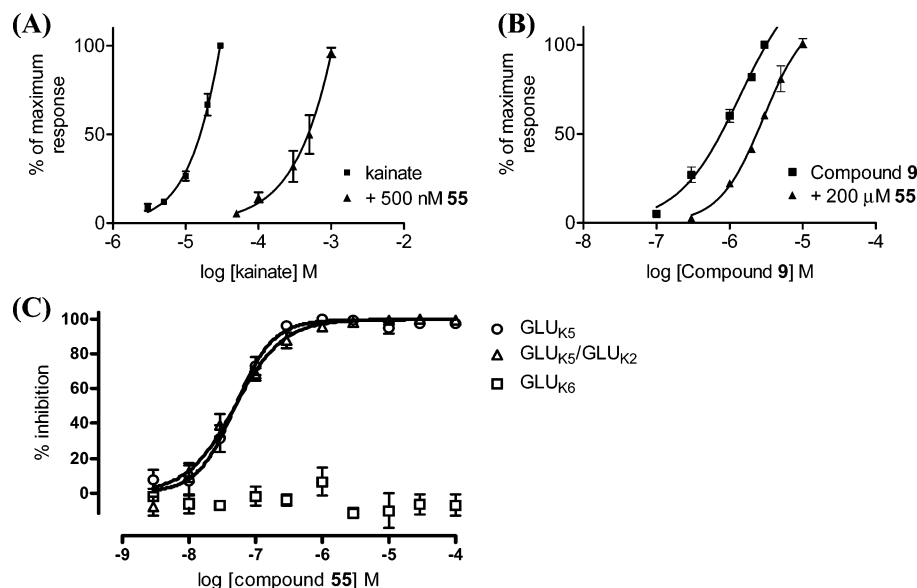


**Figure 2.** Activity of **55** on native AMPA and kainate receptors expressed on neonatal rat spinal cord and cloned kainate receptor subunits. (A) Concentration–response curves for kainate on the dorsal root in the absence and presence of 500 nM **55**. The apparent  $K_D$  value was  $18 \pm 4$  nM ( $n = 3$ ; mean  $\pm$  SEM). (B) Concentration–response curves for the AMPA receptor agonist **9** in the absence and presence of 200  $\mu$ M **55**, obtained by recording the ventral root response of the spinal cord. The apparent  $K_D$  value was  $83.4 \pm 4.1$   $\mu$ M ( $n = 3$ ; mean  $\pm$  SEM). (C) Inhibition of glutamate-induced calcium influx by **55** in cells expressing human  $GLU_{K5}$  (○),  $GLU_{K5}/GLU_{K2}$  (Δ), or  $GLU_{K6}$  (□) receptors.

**Table 2.** Summary of the Activity on Recombinant Human AMPA and Kainate Receptors of N<sup>3</sup>-Substituted Willardiine Analogues as Antagonists of Glutamate-Stimulated Ca<sup>2+</sup> Influx

compound	$GLU_{A2}$	$GLU_{K5}$	$GLU_{K5}/GLU_{K2}$	$GLU_{K5}/GLU_{K6}$	$GLU_{K6}$	$GLU_{K6}/GLU_{K2}$
<b>4</b> <sup>a</sup>	$2.5 \pm 0.3$	$37 \pm 9$	$50 \pm 10$	$28 \pm 8$	$29 \pm 14$	$135 \pm 91$
<b>11</b> <sup>b</sup>	> 300	$0.6 \pm 0.1$	$1.0 \pm 0.4$	$0.8 \pm 0.1$	> 300	> 300
<b>13</b> <sup>b</sup>	> 100	$0.12 \pm 0.03$	$0.18 \pm 0.02$	$0.12 \pm 0.01$	> 100	> 100
<b>55</b> <sup>b</sup>	> 100	$0.010 \pm 0.001$	$0.008 \pm 0.002$	> 100	> 100	> 100 <sup>c</sup>
<b>67</b> <sup>b</sup>	> 100	$0.007 \pm 0.001$	$0.005 \pm 0.001$	> 100	> 100	> 100

<sup>a</sup> Data for compound **4** represent  $IC_{50}$  values ( $\mu$ M,  $n = 3$ , mean  $\pm$  SEM) in all assays. <sup>b</sup> Data represent  $K_b$  values ( $\mu$ M,  $n = 3$ , mean  $\pm$  SEM) for  $GLU_{K5}$ ,  $GLU_{K5}/GLU_{K2}$ , and  $GLU_{K5}/GLU_{K6}$  and  $IC_{50}$  values ( $\mu$ M,  $n = 3$ , mean  $\pm$  SEM) for  $GLU_{A2}$ ,  $GLU_{K6}$ , and  $GLU_{K6}/GLU_{K2}$ . <sup>c</sup> No significant inhibition up to 30  $\mu$ M, 27  $\pm$  7% inhibition at 100  $\mu$ M.

**Ligand Docking.** QM optimized ligands were docked flexibly into the  $GLU_{A2}$  and  $GLU_{K5}$  receptors with Gold 2.2.<sup>32,33</sup> The search area was limited to a 15 Å radius sphere centered at the binding site.

Figures 3 and 4 were prepared by using Bodil<sup>30</sup> and Raster3D.<sup>34</sup>

**Effect of Substituent at the 5-Position of the Uracil Ring on Binding Affinity for  $GLU_{K5}$ .** The position of the willardiine ring is driven by the interactions with the S2-domain of  $GLU_{K5}$ , where the key interactions of the carboxylic acid group attached to the phenyl ring of **11** are with Ser674 and Thr675. The interaction with Ser674 is via a water molecule, and the carboxylate group attached to the phenyl group of **11** also interacts with the main-chain amino and side-chain hydroxyl group of Thr675, as seen in the crystal structure of **11** bound to the ligand binding core of  $GLU_{K5}$ .<sup>21</sup> Thus, the binding of 5-substituted analogues of **11** can be studied by using the crystal structure of  $GLU_{K5}$  with bound **11** and by simply replacing the hydrogen atom at the 5-position to an iodo (**12**), bromo (**36**), methyl (**34**), or fluoro (**35**) group. As seen in the crystal structure, the hydrogen atom at the 5-position of the uracil ring of **11** is located next to the oxygen atom of water molecule 148 (numbering from the X-ray structure), and there is an empty space in between the ligand, wat148, wat201, Glu426, Tyr429, Pro501, and Tyr749 (black spot in Figure 3A). This space is large enough to accommodate a water molecule, which, however, cannot hydrogen bond with any neighboring groups and thus is unorganized and not seen in the crystal structure.

Thus, neither the hydrogen atom in **11** nor the fluoro group in **35** can form favorable interactions with the surrounding groups. When the hydrogen atom is replaced by an iodo (Figure 3B) or bromo group, there is a steric clash between the ligand and the receptor. Therefore, the receptor must adjust itself in this region to be able to accommodate those groups, which in turn affects the intramolecular energy of the receptor (and the ligand binding affinity value). The 5-methyl group of **34**, however, can be perfectly accommodated by the receptor (Figure 3C). Note that the 5-iodo, 5-bromo, or 5-methyl group can replace both the wat148 and the unorganized water molecule. The rank order of potency of 5-substituted analogues of **13** on native  $GLU_{K5}$  was 5-CH<sub>3</sub> > 5-Br > 5-CF<sub>3</sub>. This rank order can be explained in a way similar to that for **11** (see above and Figure 3). The additional substituent in this series, 5-CF<sub>3</sub> (compound **57**), is fairly negatively charged due to the electronegative fluorine atoms, and thus the environment surrounding the 5-substituent, which consists of hydrophobic residues (charge  $\approx$  0) and acceptor atoms (negatively charged), is not optimal for favorable binding.

**Binding Mode of **67** in Ligand Binding Core of  $GLU_{K5}$ .** As **67** is a derivative of **55** containing an additional phenyl group at the 5-position of the thiophene ring, it is expected that it would bind in a very similar way to **55**. The better binding affinity of **67** is due to additional hydrophobic interactions with receptor. The QM optimized **67** was docked into the crystal structure of  $GLU_{K5}$  with bound antagonist ligand **55** (**55** was removed prior to docking). The docking revealed that the phenyl

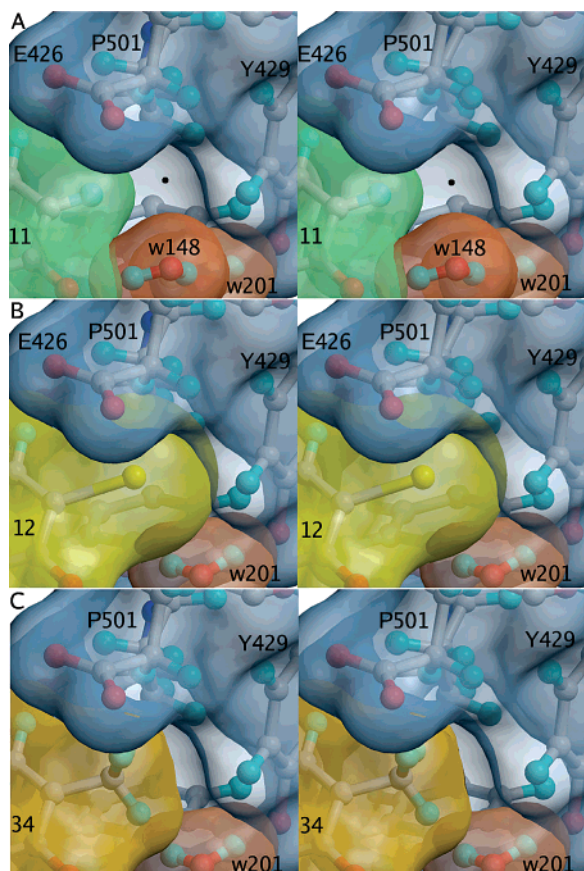


**Figure 3.** The bulkiness of substituents at the 5-position of the uracil ring of **11** and its derivatives is crucial for ligand binding affinity (figure shown in stereo). While **11** (A) leaves an empty hydrophobic cavity (black spot) that might be filled by a water molecule, the 5-iodo analogue, **12** (B), is too bulky. However, the 5-methyl group of **34** (C) is a perfect size. The surrounding residues (blue surface), water molecule (red surface), and the ligand (**11**, green surface; **12**, yellow surface; **34**, orange surface) are shown in a ball-and-stick representation.

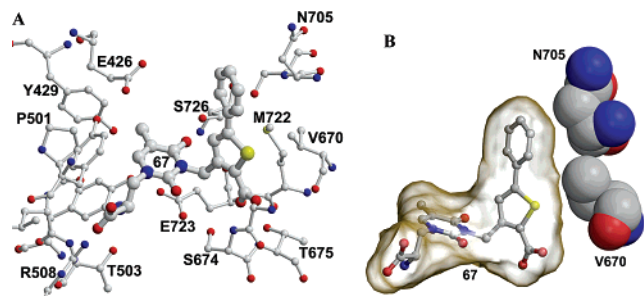


**Figure 4.** (A) Interactions of **67** with the S1S2 domain of GLUK<sub>5</sub>. The  $\alpha$ -carboxyl group forms a salt bridge with R508 and a hydrogen bond with T503, while the  $\alpha$ -amino group forms a hydrogen bond with P501, T503, and E723 (the latter via a water molecule). The carboxylic acid group attached to the thiophene ring forms hydrogen-bond interactions with S674 and T675. The 5-methyl group of **67** projects into a hydrophobic cavity formed by Y429, P501, and the CH<sub>2</sub> groups of E426. The thiophene ring of **67** forms hydrophobic interactions with V670 and M722. (B) The higher binding affinity of **67** as compared to **55** is due to additional hydrophobic interactions with residues V670 and N705.

group can form two favorable hydrophobic interactions with C <sup>$\gamma$</sup> H<sub>3</sub> of Val670 and C <sup>$\beta$</sup> H<sub>2</sub> of Asn705 (Figure 4), and this shields them from solvent. The conformation of docked **67** is practically the same as the QM optimized structure, when measuring both the root-mean-square deviation of all non-

hydrogen atoms (0.66 Å) and the QM calculated energy (QM<sup>opt</sup> – Qm<sup>docked</sup> = –2.1 kcal/mol).

**Subtype Selectivity of 67.** It was not possible to dock **67** into the GLU<sub>A2</sub> binding core conformation adopted when ATPO binds. The investigation of the binding mode of **67** in GLU<sub>A2</sub> required a receptor model of GLU<sub>A2</sub> in which the conformation is similar to that of GLU<sub>K5</sub> with **55** bound. It is likely that GLU<sub>A2</sub> can adjust itself into a conformation similar to that observed in the GLU<sub>K5</sub> crystal structure.<sup>35</sup> The crystal structure of GLU<sub>K5</sub> with bound **55**<sup>21</sup> was used as a template for the relative positions of the S1–S2 domain in the GLU<sub>A2</sub> model, while the main-chain and amino acid conformations were taken from the crystal structure of GLU<sub>A2</sub> with bound antagonist ligand ATPO.<sup>27</sup> When the binding mode of **67** in the GLU<sub>A2</sub> model is studied, it is obvious that the ligand cannot bind in a way similar to that in GLU<sub>K5</sub>, because if the docked ligand interacts with the main-chain amino and side-chain hydroxyl groups of Thr655, there is a steric clash between the ligand and the receptor, either with Leu650 or with Gly653. In particular, the bulkier Leu650 in GLU<sub>A2</sub> does not allow the thiophene ring and 5-phenyl group to be located in a position similar to that observed in GLU<sub>K5</sub> where these groups interact with Val670. Therefore, the thiophene–phenyl ring system is forced to bend toward the S1-domain of GLU<sub>A2</sub>; however, Gly653 still overlaps with the thiophene group, and thus, if this overlap is removed, the ligand would also lose partially its interactions with Thr655, which are essential for the high binding affinity in GLU<sub>K5</sub>. Thus, it is clear that the binding of **67** in GLU<sub>A2</sub> would be of much lower affinity than when this compound binds to GLU<sub>K5</sub>.

## Discussion

When tested on kainate receptors on rat dorsal root C fibers and AMPA receptors on neonatal rat motoneurons, the *N*<sup>3</sup>-(2-carboxybenzyl) derivative of willardiine, **11**, was found to be a potent and selective kainate receptor antagonist.<sup>11a,12</sup> Replacement of the benzene ring of **11** with a thiophene ring to give **13** increased potency and selectivity for kainate receptors.<sup>11b</sup> We have previously determined that the selectivity of willardiine derivatives as AMPA or kainate receptor agonists depended on the 5-substituent on the uracil ring. Indeed, 5-fluorowillardiine (**9**) was a potent and selective AMPA receptor agonist, whereas 5-iodowillardiine (**10**) was a potent and selective GLU<sub>K5</sub> kainate receptor agonist.<sup>10a–d</sup> We therefore synthesized a range of 5-substituted analogues of **11** and **13** to investigate whether 5-substitution of the uracil ring has a marked effect on antagonist potency and selectivity. Inspection of the potencies of a series of 5-substituted analogues of **11** on native GLU<sub>K5</sub>-containing kainate receptors expressed on dorsal root C fibers (see Table 1) showed that the rank order of potency was 5-CH<sub>3</sub> > 5-Br > 5-I > 5-F > 5-H, suggesting that a relatively small hydrophobic substituent was required for optimal activity. This rank order of potency is different from that observed in the agonist series of willardiine derivatives where the rank order of potency on GLU<sub>K5</sub>-containing kainate receptors expressed on dorsal root ganglion cells was 5-I > 5-Br > 5-Cl > 5-F > 5-H > 5-CH<sub>3</sub>,<sup>10a–d</sup> suggesting that the binding pocket with which the 5-substituent interacts in the closed agonist bound form of the GLU<sub>K5</sub> receptor has different structural requirements from that of the open antagonist bound form. In addition, in the agonist series, the 5-substituent increases the acidity of the uracil ring, and as the ionized form binds with higher affinity, an electron-withdrawing substituent at the 5-position of the uracil ring is favorable. However, in the antagonist series, the uracil ring cannot ionize and so electronic factors are less important.

All of the 5-substituted analogues of **11** were much more potent on GLU<sub>K5</sub>-containing kainate receptors than on native AMPA receptors; nonetheless, it is of interest to compare the rank order of potency in the antagonist series to that of 5-substituted analogues of willardiine in the agonist series. Inspection of the data for 5-substituted derivatives of **11** as antagonists of AMPA receptors expressed on motoneurons reveals the following rank order of potency: 5-F > 5-CH<sub>3</sub> > 5-Br > 5-I > 5-H, suggesting that a small substituent is preferred at the 5-position of the uracil ring. This is similar to that observed with the agonist series of willardiines where the rank order of potency was 5-F > 5-Br > 5-I > 5-H > 5-CH<sub>3</sub>.<sup>10a-d</sup> The low agonist potency of the 5-methyl-substituted analogue of willardiine on AMPA receptors is likely due to the reduced ionization of the uracil ring.

Having established that 5-methyl- or 5-bromo-substitution was optimal for GLU<sub>K5</sub> antagonist activity in the series of compounds based on **11**, we synthesized the 5-bromo and 5-methyl analogues of **13**. We also synthesized the 5-trifluoromethyl analogue **57**, as in the agonist series 5-CF<sub>3</sub> substitution of willardiine led to a potent and selective GLU<sub>K5</sub> receptor agonist and in addition the 5-CF<sub>3</sub> group is more hydrophobic than a 5-methyl group. The rank order of antagonist potency on native kainate receptors for this series of compounds was similar to that observed with the compounds based on **11**, that is, 5-CH<sub>3</sub> > 5-Br > 5-CF<sub>3</sub> > 5-H. For native AMPA receptors, the rank order of antagonist potency for 5-substituted analogues of **13** was 5-CH<sub>3</sub> > 5-H > 5-Br > 5-CF<sub>3</sub>. As in the case of 5-substituted analogues of **11**, a 5-methyl substituent was preferred to 5-Br; however, in the series of compounds based on **13**, 5-Br is less well accommodated than 5-H, although the difference is marginal.

Replacement of the thiophene ring of compounds **13** and **55** with a furan ring reduced GLU<sub>K5</sub> receptor antagonist potency, but **14** was ~3-fold more potent than the corresponding thiophene derivative **13** as an AMPA receptor antagonist. However, **55** was slightly more potent than the corresponding furan derivative **69** as an AMPA receptor antagonist. It would appear that the oxygen atom in the furan ring can form additional interactions with the ligand binding core of AMPA receptors presumably via hydrogen bonding. The thiophene ring of **13** and **55** is preferred to a furan ring for interaction with GLU<sub>K5</sub> receptors due to the ability to form better hydrophobic contacts with Val670 and Met722 in the GLU<sub>K5</sub> ligand binding core (see modeling section). The greater potency of the 5-methyl derivative **69** as compared to the parent compound **14** may be due to the favorable 5-methyl group interaction with a hydrophobic pocket in GLU<sub>K5</sub>, which offsets the reduced hydrophobic interaction with Val670 and Met722.

We have recently reported the X-ray crystal structures of **11** and **55** bound to the ligand binding core of GLU<sub>K5</sub>.<sup>21</sup> This allowed us to obtain a greater insight into the structural requirements for the optimal binding of N<sup>3</sup>-substituted willardiine derivatives to GLU<sub>K5</sub>. In addition, modeling studies allowed us to rationalize the rank order of antagonist potencies for 5-substituted analogues of **11** and **13**. Inspection of the crystal structure revealed that the 5-methyl substituent of **55** displaced a water molecule in the GLU<sub>K5</sub> receptor binding pocket and was able to fit into a cavity lined with hydrophobic substituents (Tyr429, Pro501, Tyr749, and CH<sub>2</sub> groups of Glu426), thus enhancing the binding affinity of the ligand. Modeling studies suggested that the 5-methyl substituent is the optimal size to fit into this pocket as larger substituents can only be accommodated via structural rearrangement of residues

in the binding pocket. The difference in rank order of potency for 5-substituted willardiine derivatives in the agonist and antagonist series may be due to the large degree of opening of the antagonist bound GLU<sub>K5</sub> ligand binding core. We have reported that the GLU<sub>K5</sub> ligand binding core with either **11** or **55** bound is much more open than previously described antagonist crystal structures from the AMPA or NMDA receptor families.<sup>21</sup> This large degree of opening in the antagonist bound structure of GLU<sub>K5</sub> is likely to have altered the geometry of the pocket in which the 5-substituent is incorporated.

It was apparent from the X-ray crystal structure of **55** bound to GLU<sub>K5</sub> that there was a considerable amount of space around the 4- and 5-positions of the thiophene ring. To probe the volume of this free space in the receptor, the willardiine derivatives **67** and **68** were synthesized. It was also postulated that the addition of these groups to the thiophene ring would increase the overall lipophilicity of the molecule, making them more suitable for systemic administration. Both **67** and **68** proved to be potent GLU<sub>K5</sub> receptor antagonists with **67** being more selective for GLU<sub>K5</sub> versus AMPA receptors than **68** or the parent compound **55**. The ~6-fold increase in AMPA receptor antagonist potency for **68** as compared to the parent compound **55** is likely due to additional interactions between one or both of the bromo groups and the S1-domain of the AMPA receptor. Docking of **67** into the GLU<sub>K5</sub>/**55** X-ray crystal structure suggested that the small increase in potency as compared to **55** is due to an additional hydrophobic interaction of the phenyl ring of **67** with Val670 and the CH<sub>2</sub> group of Asn705 (see modeling section). The small improvement in selectivity of **67** as compared to **55** for kainate versus AMPA receptors is likely due to a steric interaction between the 5-phenyl substituent and the leucine residue present in all AMPA receptor subunits that correspond to Val670 in GLU<sub>K5</sub>.

Characterization of compounds **11**, **13**, **55**, and **67** on cloned kainate receptors expressed in HEK293 cells suggests that these compounds have high affinity for GLU<sub>K5</sub> regardless of whether the tetrameric receptor complex is made up of GLU<sub>K5</sub> subunits alone or is a combination of GLU<sub>K5</sub> with GLU<sub>K2</sub> or GLU<sub>K6</sub>. A similar result was obtained with the decahydroisoquinoline series of GLU<sub>K5</sub> selective competitive antagonists.<sup>5</sup> However, the noncompetitive GLU<sub>K5</sub> receptor antagonist **7** (Figure 1) will only antagonize tetramers comprised of GLU<sub>K5</sub>; heteromeric GLU<sub>K5</sub> receptors are not blocked.<sup>9a</sup> Thus, antagonists such as **67** can be used in combination with **7** to help determine whether homomeric or heteromeric GLU<sub>K5</sub> kainate receptors are expressed in native tissue.

The high degree of selectivity of **67** for GLU<sub>K5</sub>-containing kainate receptors was demonstrated by the weak activity of **67** on native AMPA, NMDA, and group I mGlu receptors expressed on neonatal rat motoneurons and on cloned human AMPA and GLU<sub>K6</sub> kainate receptors. Thus, **67** can be used to investigate the role of GLU<sub>K5</sub> kainate receptors in CNS function such as synaptic plasticity and in models of neuropathic pain, epilepsy, anxiety, and migraine.

## Conclusion

We have previously reported that some N<sup>3</sup>-substituted willardiine derivatives are selective GLU<sub>K5</sub>-containing kainate receptor antagonists.<sup>2,11a,b,12</sup> This was particularly so for compounds **11** and **13**, with the latter being the most potent and selective. We have now conducted structure-activity relationship studies centered around these two compounds and have found that by 5-methyl substitution of the uracil ring we can improve both potency and selectivity for kainate receptors. In



addition, through analysis of the X-ray crystal structures of **11** and **55** docked into the ligand binding core of GLU<sub>K5</sub>, we were able to design even more potent compounds by adding substituents to the thiophene ring, thereby producing compounds **67** (ACET) and **68**, with the former being one of the most potent and selective GLU<sub>K5</sub>-containing kainate receptor antagonists identified to date. Compound **67** will be a useful pharmacological tool to study the function of GLU<sub>K5</sub>-containing kainate receptors in the CNS. Further work is in progress to investigate the usefulness of **67** for in vivo studies of CNS disorders.

## Experimental Section

**Chemistry. General Procedures.** Proton NMR spectra were measured on a Jeol NMR spectrometer at either 300.40 or 270.18 MHz. Carbon NMR spectra were run on a 300.40 MHz Jeol NMR spectrometer at 75.45 or a 270.17 MHz Jeol spectrometer at 67.94 MHz unless otherwise stated. 3-(Trimethylsilyl)propionic-2,2,3,3-*d*<sub>4</sub> acid sodium salt in D<sub>2</sub>O, or tetramethylsilane in CDCl<sub>3</sub>, DMSO-*d*<sub>6</sub>, or TFA-*d* were used as internal standards. Elemental analyses were performed by Medac Ltd., Englefield Green, UK. Melting points were determined in capillary tubes on Electrothermal IA9100 electronic melting point equipment. Determinations of optical rotation were carried out in 6 M HCl at room temperature with a wavelength of 589 nm at the University of Warwick. Thin layer chromatography was performed on Merck silica gel 60 F<sub>254</sub> plastic sheets. Silica gel for flash chromatography was silica gel 60 (220–440 mesh) from Fluka chemicals, U.K. The eluents for thin layer chromatography of amino acids included [2 (pyridine:acetic acid: water (3:8:11)):3 (*n*-butanol)] and [propan-2-ol:35% aqueous ammonia (70:30)]. Amino acids were detected by spraying plates with a 2% solution of ninhydrin in 70% ethanol. Purity of amino acids was also determined by high voltage paper electrophoresis, using pH 4 buffer and an applied voltage of 4 kV. Ion-exchange resin chromatography was carried out using Dowex 50WX8-400 acid form resin and the acetate or hydroxide form of Dowex X18-400 obtained from Aldrich Chemical Co., UK, or Biorad AG1X8 from Bio-Rad, UK. Chiral HPLC was carried out using a RSTech, ChiroSil RCA+, 150 × 4.6 column, flow rate 1.0 mL/min, detection 220 nM with a mobile phase consisting of methanol/5 mM perchloric acid (85:15). All solids were dried over P<sub>2</sub>O<sub>5</sub> in vacuo for 3 days prior to reaction. With the exception of compounds **22** and **36**, all of the amino acids synthesized were washed with anhydrous ethanol followed by diethyl ether to remove surface water. The petroleum ether utilized in each case had a boiling point range of 40–60 °C. All anhydrous reactions were conducted under argon. All reagents and dry solvents were obtained from the Aldrich Chemical Co., UK.

**5-Methyl-1-(tetrahydrofuran-2-yl)pyrimidine-2,4-dione (22).** To a suspension of thymine (**15**) (10.0 g, 79.2 mmol) in hexamethyldisilazane (72.6 mL, 317 mmol) were added chlorotrimethylsilane (10.3 mL, 79.2 mmol) followed by ammonium sulfate (0.10 g, 0.7 mmol) under a dry argon atmosphere with vigorous exclusion of moisture. The mixture was heated under reflux conditions for 18 h and then concentrated under reduced pressure (1 mmHg, 60 °C) to leave a colorless oil, which was dissolved in dry acetonitrile (50 mL) under a dry argon atmosphere. To this was added 2-acetoxytetrahydrofuran (**21**) (12.36 g, 95.04 mmol), and the mixture was stirred at room temperature for 18 h. The mixture was concentrated under reduced pressure, and the residue was purified using silica gel chromatography, eluting with ethyl acetate/petroleum ether on a gradient elution system [(3:2)–(4:1)] to give **22** (8.37 g, 54%) as a white solid, which was further purified by crystallization from methanol to give clear prisms. mp 181–182 °C; lit. mp 182–183 °C;<sup>14</sup> <sup>1</sup>H NMR (DMSO-*d*<sub>6</sub>, 270.17 MHz) δ 1.80 (d, *J* = 1.0 Hz, HCCCH<sub>3</sub>), 1.89–2.04 (m, 3H, CH<sub>2</sub>CH<sub>2</sub> + CH<sub>2</sub>CH<sub>2</sub>), 2.16–2.28 (m, 1H, CH<sub>2</sub>CH<sub>2</sub>), 3.76–3.84 (m, 1H, CHOCH<sub>2</sub>), 4.13–4.21 (m, 1H, CHOCH<sub>2</sub>), 5.93–5.97 (m, 1H, CHOCH<sub>2</sub>), 7.41 (d, *J* = 1.0 Hz, 1H, HCCCH<sub>3</sub>), 11.26 (br

s, 1H, NH); <sup>13</sup>C NMR (DMSO-*d*<sub>6</sub>, 67.94 MHz) δ 12.1, 24.0, 31.3, 69.0, 85.5, 109.1, 136.0, 150.4, 163.9; MS (electrospray) 195 [M – H]<sup>–</sup>.

Compounds **23** and **24** were synthesized using a procedure similar to that described for **22**; see the Supporting Information for more details.

**Methyl 3-Bromomethyl-5-phenylthiophene-2-carboxylate (46).** Benzoyl peroxide (0.04 g) was added to a solution of methyl 3-methyl-5-phenylthiophene-2-carboxylate (**45**) (11.6 g, 50.0 mmol) in carbon tetrachloride (500 mL). A 100 W lamp was used to irradiate the mixture, which subsequently heated to reflux, and NBS (8.01 g, 45.0 mmol) was added to the mixture in four equal portions over 4 h. The mixture was allowed to react for a further 2 h, cooled to room temperature, and filtered. The filtrate was concentrated under reduced pressure to a quarter of its original volume, and then extracted with water (3 × 100 mL), and once with saturated brine solution (50 mL). The organic layer was dried (MgSO<sub>4</sub>) and concentrated under reduced pressure to give **46** (14.76 g, 70–80% pure by <sup>1</sup>H NMR) as an orange colored oil, and this was used without further purification in the next step. <sup>1</sup>H NMR (CDCl<sub>3</sub>, 399.78 MHz) δ 3.91 (s, 3H, CH<sub>3</sub>Ar), 4.91 (s, 2H, CH<sub>2</sub>Br), 7.37 (s, 1H, Ar), 7.34–7.43 (m, 3H, Ph), 7.60–7.63 (m, 2H, Ph); MS (electrospray) 334 [M + Na]<sup>+</sup>.

Compounds **41**, **43**, and **48** were synthesized using a procedure similar to that described for **46**; see the Supporting Information for more details.

**3-(2-Methoxycarbonyl-5-phenylthiophene-3-yl-methyl)-5-methyl-1-(tetrahydrofuran-2-yl)pyrimidine-2,4-dione (58).** A 60% suspension of sodium hydride in mineral oil (0.67 g, 17 mmol) was added to a solution of 5-methyl-1-(tetrahydrofuran-2-yl)pyrimidine-2,4-dione (**22**) (3.0 g, 15 mmol) in anhydrous DMF (30 mL), and the mixture was stirred at room temperature under a dry argon atmosphere for 18 h. A solution of crude methyl 3-bromomethyl-5-phenylthiophene-2-carboxylate (**46**) (7.0 g, 18 mmol) in dry DMF (10 mL) was added, and the reaction mixture was stirred at room temperature for 48 h. The mixture was concentrated under reduced pressure (1 mmHg, 60 °C), and the resulting residue was suspended in ethyl acetate (100 mL) and washed with water (2 × 50 mL) and saturated brine solution (50 mL). The organic extract was dried (MgSO<sub>4</sub>), filtered, and concentrated under reduced pressure. The residue was purified using silica gel chromatography, eluting with ethyl acetate/petroleum ether (1:1) to give **58** (7.2 g, 46%) as a white solid. mp 145–146 °C; <sup>1</sup>H NMR (CDCl<sub>3</sub>, 270.17 MHz) δ 1.99 (d, *J* = 1.3 Hz, 3H, HCCCH<sub>3</sub>), 1.99–2.09 (m, 3H, CH<sub>2</sub>CH<sub>2</sub> + CH<sub>2</sub>CH<sub>2</sub>), 2.36–2.42 (m, 1H, CH<sub>2</sub>CH<sub>2</sub>), 3.92 (s, 3H, CO<sub>2</sub>CH<sub>3</sub>), 3.94–4.03 (m, 1H, CHOCH<sub>2</sub>), 4.19–4.27 (m, 1H, CHOCH<sub>2</sub>), 5.56 (s, 2H, CH<sub>2</sub>Ar), 6.04–6.08 (m, 1H, CHOCH<sub>2</sub>), 6.94 (s, 1H, Ar), 7.20 (d, *J* = 1.3 Hz, 1H, HCCCH<sub>3</sub>), 7.37–7.40 (m, 3H, Ph), 7.53–7.57 (m, 2H, Ph); <sup>13</sup>C NMR (CDCl<sub>3</sub>, 67.94 MHz) δ 13.5, 24.1, 32.9, 40.0, 52.0, 77.0, 87.5, 109.4, 123.7, 126.1, 126.2, 128.7, 128.9, 133.2, 133.5, 145.8, 148.9, 150.7, 162.7, 163.4; MS (electrospray) 449 [M + Na]<sup>+</sup>.

Compounds **27**, **28**, **49**, **50**, **51**, **59**, and **60** were synthesized using a procedure similar to that described for **58**; see the Supporting Information for more details.

**3-(2-Carboxy-5-phenylthiophene-3-yl-methyl)-5-methyl-1-(tetrahydrofuran-2-yl)pyrimidine-2,4-dione (61).** A solution of lithium hydroxide monohydrate (0.62 g, 15 mmol) in water (30 mL) was added to a solution of 3-(2-methoxycarbonyl-5-phenylthiophene-3-yl-methyl)-5-methyl-1-(tetrahydrofuran-2-yl)pyrimidine-2,4-dione (**58**) (2.9 g, 6.7 mmol) in dioxane (30 mL), and the mixture was stirred at room temperature for 18 h. The solution was acidified to pH 3 with 2 M aqueous HCl and then evaporated under reduced pressure. The residue was taken up in dichloromethane/ethanol (95:5) and washed with water (50 mL) and once with a saturated brine solution (50 mL), dried (MgSO<sub>4</sub>), and concentrated under reduced pressure to leave **61** (2.58 g, 93%) as a white solid. mp > 300 °C; <sup>1</sup>H NMR (CDCl<sub>3</sub>, 270.17 MHz) δ 1.91 (s, 3H, HCCCH<sub>3</sub>), 1.91–2.22 (m, 3H, CH<sub>2</sub>CH<sub>2</sub> + CH<sub>2</sub>CH<sub>2</sub>), 2.18–2.33 (m, 1H, CH<sub>2</sub>CH<sub>2</sub>), 3.8–3.89 (m, 1H, CHOCH<sub>2</sub>), 4.21–4.28 (m, 1H, CHOCH<sub>2</sub>), 5.29 (s, 2H, CH<sub>2</sub>Ar), 5.98–6.01 (m, 1H,

CHOCH<sub>3</sub>), 7.09 (s, 1H, Ar), 7.35–7.46 (m, 3H, Ph), 7.56 (s, 1H, HCCCH<sub>3</sub>), 7.65–7.69 (m, 2H, Ph), 13.2 (br s, 1H, CO<sub>2</sub>H); MS (electrospray) 411 [M + H]<sup>+</sup>.

Compounds **29**, **30**, **62**, and **63** were synthesized by a procedure similar to that described for **61**. The carboxylic acids **52**, **53**, and **54** were synthesized by hydrolysis of the *t*-butyl ester. See the Supporting Information for more details.

**3-(2-Carboxy-5-phenylthiophene-3-yl-methyl)-5-methylpyrimidine-2,4-dione (64)**. A solution of 3-(2-carboxy-5-phenylthiophene-3-yl-methyl)-5-methyl-1-(tetrahydrofuran-2-yl)pyrimidine-2,4-dione (**61**) (2.51 g, 6.09 mmol) in TFA (50 mL) was stirred for 48 h at room temperature. The mixture was concentrated under reduced pressure to leave a dark residue, which was suspended in diethyl ether (50 mL) and filtered. The solid was washed with diethyl ether (2 × 50 mL) and air-dried to give **64** (1.94 g, 93%) as a pink solid. mp >300 °C; <sup>1</sup>H NMR (DMSO-*d*<sub>6</sub>, 270.17 MHz) δ 1.84 (s, 3H, HCCCH<sub>3</sub>), 5.26 (s, 2H, CH<sub>2</sub>Ar), 7.06 (s, 1H, HCCCH<sub>3</sub>), 7.38–7.46 (m, 4H, Ph), 7.66–7.69 (m, 2H, Ar + Ph), 11.06 (d, *J* = 5.9 Hz, 1H, NH); MS (electrospray) 343 [M + H]<sup>+</sup>; 341 [M – H]<sup>–</sup>.

**(S)-1-(2-Amino-2-carboxyethyl)-3-(2-carboxy-5-phenylthiophene-3-yl-methyl)-5-methylpyrimidine-2,4-dione (67)**. A 60% suspension of sodium hydride in mineral oil (0.42 g, 11 mmol) was added to a solution of 3-(2-carboxy-5-phenylthiophene-3-yl-methyl)pyrimidine-2,4-dione (**64**) (1.64 g, 4.79 mmol) in dry DMF (170 mL) and stirred at room temperature for 18 h. (*S*)-3-(*t*-Butoxycarbonylamino)oxetan-2-one (**33**) (0.90 g, 4.8 mmol) was added, and the mixture was stirred at room temperature for 48 h. The mixture was evaporated under reduced pressure (1 mmHg, 60 °C), and 2 M aqueous HCl was added (50 mL). The mixture was evaporated under reduced pressure, and the residue was suspended in water (10 mL) and applied to Dowex 50WX8-400 ion-exchange resin (H<sup>+</sup> form) (0.25 mmol of cation/mL of resin; 100 mL) with stirring for 30 min. The mixture was then applied to a column containing an equivalent volume of Dowex 50WX8-400 resin and eluted with water until no ninhydrin positive fractions were observed, THF/water (1:1), until the eluate was colorless, and then elution was continued with 1 M aqueous pyridine. The ninhydrin positive fractions of the 1 M aqueous pyridine eluate were combined and evaporated to dryness under reduced pressure. Crystallization of the residue from water yielded **67** (0.84 g, 38%) as a white solid. To further purify the final product, it was twice stirred in hot dioxane, filtered, and air-dried. mp 275–278 °C (dec); [α]<sup>25</sup><sub>D</sub> = +1.0 (*c* 0.455, 6 M HCl); ee >99% as determined by chiral HPLC; <sup>1</sup>H NMR (TFA-*d*, 270.17 MHz) δ 2.12 (s, 3H, HCCCH<sub>3</sub>), 4.66–4.84 (m, 2H, CHCH<sub>2</sub>), 5.05–5.02 (m, 1H, CHCH<sub>2</sub>), 5.73 (s, 2H, CH<sub>2</sub>Ar), 7.09 (s, 1H, Ar), 7.41–7.59 (m, 6H, Ph + HCCCH<sub>3</sub>); MS (electrospray) 452 [M + Na]<sup>+</sup>.

**(S)-1-(2-Amino-2-carboxyethyl)-3-(2-carboxybenzyl)-5-methylpyrimidine-2,4-dione (34)**. Following a procedure similar to that described for **67**, a 60% suspension of sodium hydride in mineral oil (0.44 g, 11 mmol), 3-(2-carboxybenzyl)-5-methylpyrimidine-2,4-dione (**31**) (1.43 g, 5.51 mmol), and (*S*)-3-(*t*-butoxycarbonylamino)oxetan-2-one (**33**) (1.03 g, 5.51 mmol) yielded **34** (1.11 g, 58%) as a white solid. mp 217–221 °C (dec); [α]<sup>25</sup><sub>D</sub> = –7.2 (*c* 0.572, 6 M HCl); ee >99% as determined by chiral HPLC; <sup>1</sup>H NMR (D<sub>2</sub>O + NaOD [pH = 12], 270.17 MHz) δ 3.60 (dd, *J*<sub>AX</sub> + *J*<sub>BX</sub> = 14.2 Hz, 1H, CHCH<sub>2</sub>), 3.89 (dd, *J*<sub>BA</sub> = 13.9 Hz, *J*<sub>BX</sub> = 7.6 Hz, 1H, CHCH<sub>2</sub>), 4.05 (dd, *J*<sub>AB</sub> = 13.9 Hz, *J*<sub>AX</sub> = 5.9 Hz, 1H, CHCH<sub>2</sub>), 5.34 (s, 2H, CH<sub>2</sub>Ar), 6.96–6.99 (m, 1H, Ph), 7.32–7.35 (m, 2H, Ph), 7.49 (s, 1H, HCCCH<sub>3</sub>), 7.53–7.56 (m, 1H, Ph); <sup>13</sup>C NMR (D<sub>2</sub>O + NaOD [pH = 12], 67.94 MHz) δ 14.9, 46.5, 56.3, 58.0, 112.7, 127.5, 129.9, 130.6, 132.3, 135.6, 140.7, 144.6, 155.5, 168.9, 180.0, 182.4; MS (electrospray) 348 [M + H]<sup>+</sup>; HRMS *m/z* (M + Na)<sup>+</sup> calculated for C<sub>16</sub>H<sub>18</sub>N<sub>3</sub>O<sub>6</sub>, 348.1190; found, 348.1188.

**(S)-1-(2-Amino-2-carboxyethyl)-3-(2-carboxybenzyl)-5-fluoropyrimidine-2,4-dione (35)**. Following a procedure similar to that described for **67**, 3-(2-carboxybenzyl)-5-fluoropyrimidine-2,4-dione (**32**) (0.48 g, 1.8 mmol), a 60% suspension of sodium hydride in mineral oil (0.14 g, 3.6 mmol), and (*S*)-3-(*t*-butoxycarbonylamino)oxetan-2-one (**33**) (0.34 g, 1.8 mmol) gave **35** (0.22 g, 34%) as

white needles. mp 195–197 °C (dec); [α]<sup>25</sup><sub>D</sub> = –8.4 (*c* 0.105, 6 M HCl); ee >99% as determined by chiral HPLC; <sup>1</sup>H NMR (TFA-*d*, 270.17 MHz) δ 4.66 (dd, *J*<sub>BA</sub> = 15.8 Hz, *J*<sub>BX</sub> = 5.9 Hz, 1H, CHCH<sub>2</sub>), 4.72 (dd, *J*<sub>AB</sub> = 15.8 Hz, *J*<sub>AX</sub> = 3.0 Hz, 1H, CHCH<sub>2</sub>), 5.01 (dd, *J*<sub>AX</sub> + *J*<sub>BX</sub> = 8.3 Hz, 1H, CHCH<sub>2</sub>), 5.81 (s, 2H, CH<sub>2</sub>Ph), 7.15 (d, *J* = 7.6 Hz, 1H, Ph), 7.47–7.53 (m, 1H, Ph), 7.60 (dt, *J* = 7.6 Hz, *J* = 1.3 Hz, 1H, Ph), 7.86 (d, *J* = 4.62, 1H, HCCFCO), 8.24 (dd, *J* = 7.6 Hz, *J* = 1.3 Hz, 1H, Ph); <sup>13</sup>C NMR (D<sub>2</sub>O + DCl [pH 1], 67.94 MHz) δ 46.9, 52.1, 54.7, 129.1, 130.7, 132.1, 132.3, 132.8, 133.7, 136.0, 138.7, 154.5, 162.1 (d, *J* = 25.4 Hz), 171.8, 174.0; MS (electrospray) 352.1 [M + H]<sup>+</sup>; 374.1 [M + Na]<sup>+</sup>.

**(S)-1-(2-Amino-2-carboxyethyl)-3-(2-carboxythiophene-3-yl-methyl)-5-methylpyrimidine-2,4-dione (55)**. Following a procedure similar to that described for **67**, a 60% suspension of sodium hydride in mineral oil (0.33 g, 8.3 mmol), 3-(2-carboxythiophene-3-yl-methyl)-5-methylpyrimidine-2,4-dione (**52**) (1.10 g, 4.14 mmol), and (*S*)-3-(*t*-butoxycarbonylamino)oxetan-2-one (**33**) (0.77 g, 4.1 mmol) yielded **55** (0.56 g, 39%) as a white solid; mp 226–228 °C (dec); [α]<sup>25</sup><sub>D</sub> = –7.6 (*c* 0.345, 6 M HCl); ee >99% as determined by chiral HPLC; <sup>1</sup>H NMR (D<sub>2</sub>O [+DCl, pH 1], 399.78 MHz) δ 1.92 (d, *J* = 1.1 Hz, 3H, HCCCH<sub>3</sub>), 4.35 (dd, *J*<sub>BA</sub> = 15.0 Hz, *J*<sub>BX</sub> = 6.6 Hz, 1H, CH<sub>2</sub>CH), 4.45 (dd, *J*<sub>AB</sub> = 15.0 Hz, *J*<sub>AX</sub> = 5.1 Hz, 1H, CH<sub>2</sub>CH), 4.56 (dd, *J*<sub>AX</sub> + *J*<sub>BX</sub> = 11.7 Hz, 1H, CH<sub>2</sub>CH), 5.40 (s, 2H, CH<sub>2</sub>Ar), 6.82 (d, *J* = 5.5 Hz, 1H, Ar), 7.58 (d, *J* = 1.1 Hz, HCCCH<sub>3</sub>), 7.64 (d, *J* = 5.5 Hz, 1H, Ar); <sup>13</sup>C NMR (D<sub>2</sub>O [+DCl, pH 1], 100.54 MHz) δ 29.0, 36.7, 39.8, 98.9, 115.7, 115.6, 120.6, 128.8, 128.9, 132.3, 140.7, 153.2, 153.3, 156.8; MS (electrospray) 354 (M + H)<sup>+</sup>; 376 (M + Na)<sup>+</sup>; 352 (M – H)<sup>–</sup>.

**(S)-1-(2-Amino-2-carboxyethyl)-5-bromo-3-(2-carboxythiophene-3-yl-methyl)pyrimidine-2,4-dione (56)**. Following a procedure similar to that described for **67**, 5-bromo-3-(2-carboxythiophene-3-yl-methyl)-5-pyrimidine-2,4-dione (**53**) (3.00 g, 9.06 mmol), a 60% suspension of sodium hydride in mineral oil (0.72 g, 18 mmol), and (*S*)-3-(*t*-butoxycarbonylamino)oxetan-2-one (**33**) (1.52 g, 8.15 mmol) gave **56** (2.23 g, 59%) as a white solid; mp 192–196 °C (dec); [α]<sup>25</sup><sub>D</sub> = +3.2 (*c* 0.538, 6 M HCl); ee >98% as determined by chiral HPLC; <sup>1</sup>H NMR (TFA-*d*, 270.17 MHz) δ 4.70 (dd, *J*<sub>BA</sub> = 15.8 Hz, *J*<sub>BX</sub> = 6.3 Hz, 1H, CHCH<sub>2</sub>), 4.83 (dd, *J*<sub>AB</sub> = 15.8 Hz, *J*<sub>AX</sub> = 3.0 Hz, 1H, CHCH<sub>2</sub>), 5.02 (dd, *J*<sub>AX</sub> + *J*<sub>BX</sub> = 8.6 Hz, 1H, CHCH<sub>2</sub>), 5.76 (s, 2H, CH<sub>2</sub>Ar), 6.93 (d, *J* = 5.3 Hz, 1H, Ar), 7.67 (d, *J* = 5.3 Hz, 1H, Ar), 8.06 (s, 1H, HCCBr); MS (electrospray) 418 [M + H]<sup>+</sup>; 420 [M + H]<sup>+</sup>; 416 [M – H]<sup>–</sup>; 418 [M – H]<sup>–</sup>.

**(S)-1-(2-Amino-2-carboxyethyl)-3-(2-carboxythiophene-3-yl-methyl)-5-trifluoromethylpyrimidine-2,4-dione (57)**. Following a procedure similar to that described for **67**, 3-(2-carboxythiophene-3-yl-methyl)-5-trifluoromethylpyrimidine-2,4-dione (**54**) (2.00 g, 6.25 mmol), a 60% suspension of sodium hydride in mineral oil (0.52 g, 13 mmol), and (*S*)-3-(*t*-butoxycarbonylamino)oxetan-2-one (**33**) (1.17 g, 6.25 mmol) gave **57** (1.25 g, 49%) as a white solid. mp 187–190 °C (dec); [α]<sup>25</sup><sub>D</sub> = –4.5 (*c* 0.51, 6 M HCl); ee >99% as determined by chiral HPLC; <sup>1</sup>H NMR (TFA-*d*, 270.17 MHz) δ 4.77 (dd, *J*<sub>BA</sub> = 15.8 Hz, *J*<sub>BX</sub> = 6.3 Hz, 1H, CH<sub>2</sub>CH), 4.87 (dd, *J*<sub>AB</sub> = 15.8 Hz, *J*<sub>AX</sub> = 3.5 Hz, 1H, CH<sub>2</sub>CH), 5.05 (dd, *J*<sub>AX</sub> + *J*<sub>BX</sub> = 9.6 Hz, 1H, CH<sub>2</sub>CH), 5.73 (s, 2H, CH<sub>2</sub>Ar), 6.96 (d, *J* = 5.3 Hz, 1H, Ar), 7.66 (d, *J* = 5.3 Hz, 1H, Ar), 8.23 (s, 1H, HCCCF<sub>3</sub>); MS (electrospray) 408 [M + H]<sup>+</sup>; 406 [M – H]<sup>–</sup>.

**(S)-1-(2-Amino-2-carboxyethyl)-3-(2-carboxy-4,5-dibromothiophene-3-yl-methyl)-5-methylpyrimidine-2,4-dione (68)**. Following a procedure similar to that described for **67**, 3-(2-carboxy-4,5-dibromothiophene-3-yl-methyl)-5-methylpyrimidine-2,4-dione (**65**) (4.67 g, 11 mmol), a 60% suspension of sodium hydride in mineral oil (0.97 g, 24.2 mmol), and (*S*)-3-(*t*-butoxycarbonylamino)oxetan-2-one (**33**) (2.06 g, 11 mmol) gave **68** as a white solid (0.68 g, 12%); mp 210–213 °C (dec); [α]<sup>25</sup><sub>D</sub> = +3.8 (*c* 0.495, 6 M HCl); ee >99% as determined by chiral HPLC; <sup>1</sup>H NMR (TFA-*d*, 399.78 MHz) δ 2.02 (s, 3H, HCCCH<sub>3</sub>), 4.62–4.70 (m, 1H, HCCCH<sub>2</sub>), 4.79–4.86 (m, 1H, HCCCH<sub>2</sub>), 4.96–5.06 (m, 1H, HCCCH<sub>2</sub>), 5.71 (s, 2H, CH<sub>2</sub>Ar), 7.50 (s, 1H, HCCCH<sub>3</sub>); MS (electrospray) 510 [M – H]<sup>–</sup>.

(*S*)-1-(2-Amino-2-carboxyethyl)-3-(2-carboxyfuran-3-yl-methyl)-5-methylpyrimidine-2,4-dione (**69**). Following a procedure similar to that described for **67**, 3-(2-carboxyfuran-3-yl-methyl)-5-methylpyrimidine-2,4-dione (**66**) (1.03 g, 4.12 mmol), a 60% suspension of sodium hydride in mineral oil (0.33 g, 8.2 mmol), and (*S*)-3-(*t*-butoxycarbonylamino)oxetan-2-one (**33**) (0.77 g, 4.1 mmol) gave **69** (0.48 g, 35%) as a white solid; mp 225–227 °C (dec);  $[\alpha]_D^{25} = -9.5$  (*c* 0.595, 6 M HCl); ee >99% as determined by chiral HPLC;  $^1\text{H NMR}$  (TFA-*d*, 399.78 MHz)  $\delta$  2.10 (s, 3H, HCCCH<sub>3</sub>), 4.66 (dd,  $J_{\text{BA}} = 15.6$  Hz,  $J_{\text{BX}} = 6.3$  Hz, 1H, CH<sub>2</sub>CH), 4.78 (dd,  $J_{\text{AB}} = 15.6$  Hz,  $J_{\text{AX}} = 2.9$  Hz, 1H, CH<sub>2</sub>CH), 5.00 (dd,  $J_{\text{AX}} + J_{\text{BX}} = 8.8$  Hz, 1H, CH<sub>2</sub>CH), 5.60 (s, 2H, CH<sub>2</sub>Ar), 6.50 (s, 1H, Ar), 7.54 (s, 1H, HCCCH<sub>3</sub>), 7.64 (s, 1H, Ar); MS (electrospray) 336 [M - H]<sup>-</sup>; 337 [M]<sup>-</sup>; 338 [M + H]<sup>+</sup>; 360 [M + Na]<sup>+</sup>.

(*S*)-1-(2-Amino-2-carboxyethyl)-5-bromo-3-(2-carboxybenzyl)-pyrimidine-2,4-dione (**36**). To a solution of (*S*)-1-(2-amino-2-carboxyethyl)-3-(2-carboxybenzyl)pyrimidine-2,4-dione (**11**) (0.15 g, 0.43 mmol) in water/acetic acid (1:1; 10 mL) was added a 2 M solution of bromine in acetic acid (0.11 mL), and the mixture was stirred at room temperature for 30 min. The reaction had not gone to completion, as deduced by TLC, and a further aliquot of bromine solution was added (0.33 mL). The mixture was stirred for a further 18 h and then concentrated under reduced pressure. The remaining residue was suspended in water (5 mL) and applied to Dowex 50WX8-400 ion-exchange resin (H<sup>+</sup> form, 0.25 mmol of cation/mL of resin; 5 mL) with stirring for 30 min. The mixture was then applied to a column containing an equivalent volume of Dowex 50WX8-400 resin (H<sup>+</sup> form) and eluted with water until no ninhydrin positive fractions were observed, THF/water (1:1), until the eluate was colorless, and then elution was continued with 1 M aqueous pyridine. The ninhydrin positive fractions of the 1 M aqueous pyridine eluate were combined and evaporated to dryness under reduced pressure.

Crystallization of the residue from water yielded **36** (0.11 g, 42%) as a white solid. mp 184–185 °C (dec);  $[\alpha]_D^{25} = 6.9$  (*c* 0.11, 6 M HCl); ee 92% as determined by chiral HPLC;  $^1\text{H NMR}$  (TFA-*d*, 270.17 MHz)  $\delta$  4.72 (dd,  $J_{\text{BA}} = 15.8$  Hz,  $J_{\text{BX}} = 5.9$  Hz, 1H, CH<sub>2</sub>-CH), 4.85 (dd,  $J_{\text{AB}} = 15.8$  Hz,  $J_{\text{AX}} = 3.0$  Hz, 1H, CH<sub>2</sub>CH), 5.05 (dd,  $J_{\text{AX}} + J_{\text{BX}} = 9.2$  Hz, 1H, CH<sub>2</sub>CH), 5.83 (s, 2H, CH<sub>2</sub>Ph), 7.14 (d,  $J = 7.6$  Hz, 1H, Ph), 7.62–7.48 (m, 2H, Ph), 8.08 (s, 1H, HCCBrCO), 8.24 (dd,  $J = 1.3$  Hz,  $J = 7.6$  Hz, 1H, Ph); MS (electrospray) 412.3 [M]<sup>+</sup>.

**Electrophysiology. Antagonism of Kainate Responses on Dorsal Root C-Fibers by Novel Willardiine Derivatives.** Experiments to test the antagonist effect of the novel compounds at GLU<sub>K5</sub>-containing kainate receptors were conveniently carried out on kainate-induced responses on isolated dorsal roots from non-anaesthetized 1–5-day-old rats, as described in detail previously.<sup>12</sup> To prevent desensitization of kainate receptors, the dorsal root was superfused with 1 mg mL<sup>-1</sup> Concanavalin A for 20 min after a 20 min exposure to glucose-free superfusion medium. Standard superfusion medium was then applied throughout the experiments. This allowed measurement of depolarizations evoked by the exogenously applied agonist, kainate (1 min applications). Non-cumulative, nonsequential concentration–response curves were constructed for kainate in the absence and presence of the antagonist (30 min preincubation). The EC<sub>50</sub> values (10–15 μM) for kainate-induced depolarization of the dorsal root determined in assays of antagonists did not differ significantly from previously reported values.<sup>12,24a,25</sup>

**Characterization of AMPA Receptor Antagonists.** Hemisected spinal cords from non-anaesthetized 1–5-day-old rats killed by cervical dislocation were prepared and used according to the reported method.<sup>38</sup> To assess AMPA receptor antagonist activity, the ability of the compounds to block the fast component of the dorsal root-evoked ventral root potential (fDR-VRP) in the neonatal rat hemisected spinal cord preparation was measured, as described in detail previously.<sup>12,26</sup> Concentration–response curves were constructed for test antagonists (5 min applications), in the presence of 2 mM MgSO<sub>4</sub>/50 μM (*R*)-2-amino-5-phosphopentanoic acid

(30 min preincubation), to block NMDA receptors. Results are expressed as mean ± SEM, *n* = 3.

To further characterize the AMPA receptor antagonist activity of compounds **55** and **67**, experiments were performed on AMPA receptors expressed on motoneurons in the hemisected neonatal rat spinal cord preparation in the presence of tetrodotoxin (TTX, 10 μM for 2 min, then 0.1 μM continuously) to block action-potential-dependent release. No electrical stimulation was applied, thus allowing measurement of depolarizations evoked by an exogenously applied AMPA receptor agonist.<sup>26</sup> Noncumulative concentration–response curves were obtained for the selective AMPA receptor agonist **9** (1 min applications) in the absence and presence of 200 μM **55** or **67** (30 min preincubation), allowing dose ratios to be calculated. The *K<sub>D</sub>* values for antagonism of **9** by **55** or **67** were calculated from the dose ratios using the Gaddum–Schild equation.

**Characterization of 55 and 67 on NMDA and Group I Metabotropic Glutamate Receptors Expressed on Neonatal Rat Motoneurons.** Experiments performed to investigate the effect of **55** and **67** on receptors expressed on motoneurons in the hemisected neonatal rat spinal cord preparation were carried out in the presence of tetrodotoxin (TTX, 10 μM for 2 min, then 0.1 μM continuously) to block action-potential-dependent release. No electrical stimulation was applied, thus allowing measurement of depolarizations evoked by exogenously applied agonists.<sup>26</sup> In experiments to determine the antagonist selectivity of **55** and **67**, medium containing approximately equi-effective concentrations of either **1** (0.7 μM), NMDA (10 μM), or DHPG (20 μM) was applied for 1 min, in the absence and presence of **55** (10 μM; 30 min preincubation) or **67** (1 μM; 30 min preincubation).

**Calcium Fluorescence Assays Using Recombinant Human AMPA and Kainate Receptor Subtypes. AMPA Receptor Assays.** HEK293 cells stably expressing human AMPA receptors were seeded into poly-D-lysine-coated 96-well plates (Becton Dickinson Labware, Bedford, MA) 1 or 2 days prior to experiments at 60 000 cells/well (1 day) or 30 000 cells/well (2 day). Cells were washed three times with 100 μL of assay buffer composed of Hanks Balanced Salt Solution without phenol red (Invitrogen) with 20 mM HEPES and 3.7 mM CaCl<sub>2</sub> added (final [CaCl<sub>2</sub>] = 5 mM). Plates were then incubated for 2–3 h at room temperature in 40 μL of assay buffer with 8 μM Fluo3-AM dye (Molecular Probes Inc., Eugene, OR). Following dye incubation, cells were rinsed once with 100 μL of assay buffer. Finally, 50 μL of assay buffer, which included the AMPA receptor potentiator LY392098 (10 μM; to prevent desensitization of AMPA receptors), was added to wells, and fluorescence was measured using a fluorometric imaging plate reader (FLIPR; Molecular Devices, Sunnyvale, CA). The FLIPR added a first addition of 50 μL of LY392098-containing assay buffer, followed by a second addition of 100 μL of LY392098-containing buffer 3 min later. **55** or **67** was added in the absence of agonist during the first addition, and in the presence of 100 μM glutamate during the second addition.

**Kainate Receptor Assays.** All receptor clones were stably expressed in HEK293 cells. The GLU<sub>K5(Q)</sub>/GLU<sub>K2</sub> cell line was created by retroviral infection of cDNA coding for the human GLU<sub>K2</sub> subunit (EAA2; Allelix Biopharmaceuticals) into the GLU<sub>K5(Q)</sub>-expressing cell line using the pMNLZRS/IB retroviral expression vector. HEK293 cell lines stably expressing a cloned GLU<sub>K5(Q)</sub><sup>39</sup> or GLU<sub>K6(Q)</sub> receptor subunit,<sup>40</sup> or coexpressing GLU<sub>K5(R)</sub> and GLU<sub>K6(Q)</sub><sup>5c</sup>, or GLU<sub>K6(Q)</sub> and GLU<sub>K2</sub>,<sup>41</sup> have been previously described. Kainate receptor expression levels for all transfected cell lines have been previously determined in our laboratory by saturation binding of [<sup>3</sup>H]kainate to intact cells. *B*<sub>max</sub> values for specific [<sup>3</sup>H]kainate binding are GLU<sub>K5(Q)</sub>, 1.7 ± 0.5 pmol/mg; GLU<sub>K5(R)</sub>/6(Q), 8 ± 2 pmol/mg; GLU<sub>K5(Q)</sub>/GLU<sub>K2</sub>, 0.6 ± 0.1 pmol/mg; GLU<sub>K6(Q)</sub>, 2.7 ± 0.3 pmol/mg; GLU<sub>K6(Q)</sub>/GLU<sub>K2</sub>, 1.7 ± 0.3 pmol/mg.<sup>42</sup> To address the possibility that changes in receptor expression levels over time could influence experimentally determined IC<sub>50</sub> values, the EC<sub>50</sub> value for glutamate and the IC<sub>50</sub> values for routinely used control antagonists such as **4** (Figure 1) were continuously monitored, and no significant drift in these values

was ever observed. Additionally, cells were never passaged more than 20 times.

Cell growth and ion influx studies using a FLIPR were carried out exactly as described previously, in the presence of concanavalin A.<sup>12</sup> The antagonist **55** or **67** was added in the absence of agonist during the first addition, and in the presence of 100  $\mu$ M glutamate during the second addition. Concentration–response curves for **55** and **67** were analyzed using GraphPad Prism 3.02 software (San Diego, CA), with slope factor fixed at 1, and top and bottom fixed at 100% and 0% inhibition, respectively. The dissociation constant ( $K_b$ ) was calculated according to the Cheng–Prusoff equation<sup>43</sup> from the IC<sub>50</sub> value for inhibiting 100  $\mu$ M glutamate-induced calcium influx.

**Acknowledgment.** We would like to thank the following organizations for funding this work: BBSRC, UK and the Brain Research Center of the 21st Century Frontier Research Program funded by the Korean Ministry of Science and Technology. We also would like to thank Louise C. Argent and Anna Thom from Tocris Bioscience for providing chiral HPLC and mass spectrometry data. We thank Dr. Richard Sessions (Department of Biochemistry, University of Bristol) for access to the docking software and the Centre for Computational Chemistry (University of Bristol) for access to their computing resources. O.T.P. was supported by the Academy of Finland. This research was funded in part by the Intramural Research Program of the NIH, National Institute of Child Health and Human Development.

**Supporting Information Available:** Elemental analyses for intermediates and final compounds. Experimental and spectroscopic data for intermediates. This material is available free of charge via the Internet at <http://pubs.acs.org>.

## References

- (a) Bettler, B.; Mülle, C. Neurotransmitter receptors. 2. AMPA and kainate receptors. *Neuropharmacology* **1995**, *34*, 123–139. (b) Fletcher, E. J.; Lodge, D. New developments in the molecular pharmacology of  $\alpha$ -amino-3-hydroxy-5-methyl-4-isoxazolepropionate and kainate receptors. *Pharmacol. Ther.* **1996**, *70*, 65–89. (c) Bleakman, D.; Lodge, D. Neuropharmacology of AMPA and kainate receptors. *Neuropharmacology* **1998**, *37*, 1187–1204. (d) Chittajallu, R.; Braithwaite, S. P.; Clarke, V. R.; Henley, J. M. Kainate receptors: subunits, synaptic localization and function. *Trends Pharmacol. Sci.* **1999**, *20*, 26–35.
- (a) Watkins, J. C.; Jane, D. E. The glutamate story. *Br. J. Pharmacol.* **2006**, *147*, S100–S108. (b) Jane, D. E. Antagonists acting at the NMDA receptor complex: potential for therapeutic applications. In *Glutamate and GABA Receptors and Transporters*; Krosggaard-Larsen, P., Egebjerg, J., Schousboe, A., Eds.; Taylor and Francis: London, 2002; pp 69–98. (c) Bräuner-Osborne, H.; Egebjerg, J.; Nielsen, E. O.; Madsen, U.; Krosggaard-Larsen, P. Ligands for glutamate receptors: design and therapeutic prospects. *J. Med. Chem.* **2000**, *43*, 2609–2645. (d) Kew, J. N. C.; Kemp, J. A. Ionotropic and metabotropic glutamate receptor structure and pharmacology. *Psychopharmacology* **2005**, *179*, 4–29.
- Lodge, D.; Dingledine, R. Ionotropic Glutamate Receptors. *The IUPHAR Compendium of Receptor Characterization and Classification*, 2nd ed.; IUPHAR Media Ltd.: London, 2001.
- (a) Sheardown, M.; Nielsen, E.; Hansen, A.; Jacobsen, P.; Honore, T. 2,3-Dihydroxy-6-nitro-7-sulphamoyl-benzo(F)quinoxaline: A neuroprotectant for cerebral ischemia. *Science* **1990**, *247*, 571–574. (b) Watkins, J. C.; Krosggaard-Larsen, P.; Honoré, T. Structure-activity relationships in the development of excitatory amino acid receptor agonists and competitive antagonists. *Trends Pharmacol. Sci.* **1990**, *11*, 25–33.
- (a) Clarke, V. R.; Ballyk, B. A.; Hoo, K. H.; Mandelzys, A.; Pellizzari, A.; Bath, C. P.; Thomas, J.; Sharpe, E. F.; Davies, C. H.; Ornstein, P. L.; Schoepp, D. D.; Kamboj, R. K.; Collingridge, G. L.; Lodge, D.; Bleakman, D. A hippocampal GluR5 kainate receptor regulating inhibitory synaptic transmission. *Nature* **1997**, *389*, 599–603. (b) Vignes, M.; Clarke, V. R.; Parry, M. J.; Bleakman, D.; Lodge, D.; Ornstein, P. L.; Collingridge, G. L. The GluR5 subtype of kainate receptor regulates excitatory synaptic transmission in areas CA1 and CA3 of the rat hippocampus. *Neuropharmacology* **1998**, *37*, 1269–1277. (c) Bortolotto, Z. A.; Clarke, V. R.; Delany, C. M.; Parry, M. C.; Smolders, I.; Vignes, M.; Ho, K. H.; Miu, P.; Brinton, B. T.

- Fantaske, R.; Ogden, A.; Gates, M.; Ornstein, P. L.; Lodge, D.; Bleakman, D.; Collingridge, G. L. Kainate receptors are involved in synaptic plasticity. *Nature* **1999**, *402*, 297–301. (d) Filla, S. A.; Winter, M. A.; Johnson, K. W.; Bleakman, D.; Bell, M. G.; Bleisch, T. J.; Castano, A. M.; Clemens-Smith, A.; Del Prado, M.; Dieckman, D. K.; Dominguez, E.; Escribano, A.; Ho, K. H.; Hudziak, K. J.; Katofiasc, M. A.; Martinez-Perez, J. A.; Mateo, A.; Mathes, B. M.; Mattiuz, E. L.; Ogden, A. M. L.; Phebus, L. A.; Stack, D. R.; Stratford, R. E.; Ornstein, P. L. Ethyl (3*S*,4*a**R*,6*S*,8*a**R*)-6-(4-ethoxycarbonylimidazol-1-ylmethyl)decahydroisoquinoline-3-carboxylic ester: a prodrug of a GluR5 kainate receptor antagonist active in two animal models of acute migraine. *J. Med. Chem.* **2002**, *45*, 4383–4386. (e) Dominguez, E.; Iyengar, S.; Shannon, H. E.; Bleakman, D.; Alt, A.; Arnold, B. M.; Bell, M. G.; Bleisch, T. J.; Buckmaster, J. L.; Castano, A. M.; Prado, M. D.; Escribano, A.; Filla, S. A.; Ho, K. H.; Hudziak, K. J.; Jones, C. K.; Martinez-Perez, J. A.; Mateo, A.; Mathes, B. M.; Mattiuz, E. L.; Ogden, A. M. L.; Simmons, R. M. A.; Stack, D. R.; Stratford, R. E.; Winter, M. A.; Wu, Z.; Ornstein, P. L. Two prodrugs of potent and selective GluR5 kainate receptor antagonists active in three animal models of pain. *J. Med. Chem.* **2005**, *48*, 4200–4203. (f) Weiss, B.; Alt, A.; Ogden, A. M.; Gates, M.; Dieckman, D. K.; Clemens-Smith, A.; Ho, K. H.; Jarvie, K.; Rizkalla, G.; Wright, R. A.; Calligaro, D. O.; Schoepp, D.; Mattiuz, E. L.; Stratford, R. E.; Johnson, B.; Salhoff, C.; Katofiasc, M.; Phebus, L. A.; Schenck, K.; Cohen, M.; Filla, S. A.; Ornstein, P. L.; Johnson, K. W.; Bleakman, D. Pharmacological characterization of the competitive GLU<sub>K5</sub> receptor antagonist decahydroisoquinoline LY466195 in vitro and in vivo. *J. Pharmacol. Exp. Ther.* **2006**, *318*, 772–781.
- (a) O'Neill, M. J.; Bond, A.; Ornstein, P. L.; Ward, M. A.; Hicks, C. A.; Hoo, K.; Bleakman, D.; Lodge, D. Decahydroisoquinolines: novel competitive AMPA/kainate antagonists with neuroprotective effects in global cerebral ischaemia. *Neuropharmacology* **1998**, *37*, 1211–1222. (b) Simmons, R. M. A.; Li, D. L.; Hoo, K. H.; Deverill, M.; Ornstein, P. L.; Iyengar, S. Kainate GluR5 receptor mediates the nociceptive response to formalin in the rat. *Neuropharmacology* **1998**, *37*, 25–36. (c) O'Neill, M. J.; Bogaert, L.; Hicks, C. A.; Bond, A.; Ward, M. A.; Ebinger, G.; Ornstein, P. L.; Michotte, Y.; Lodge, D. LY377770, a novel iGluR5 kainate receptor antagonist with neuroprotective effects in global and focal cerebral ischaemia. *Neuropharmacology* **2000**, *39*, 1575–1588. (d) Smolders, I.; Bortolotto, Z. A.; Clarke, V. R. J.; Warre, R.; Khan, G. M.; O'Neill, M. J.; Ornstein, P. L.; Bleakman, D.; Ogden, A.; Weiss, B.; Stables, J. P.; Ho, K. H.; Ebinger, G.; Collingridge, G. L.; Lodge, D.; Michotte, Y. Antagonists of GLU<sub>K5</sub>-containing kainate receptors prevent pilocarpine-induced limbic seizures. *Nat. Neurosci.* **2002**, *5*, 796–804.
- Sanders, J. M.; Ito, K.; Settimo, L.; Pentikainen, O. T.; Shoji, M.; Sasaki, M.; Johnson, M. S.; Sakai, R.; Swanson, G. T. Divergent pharmacological activity of novel marine-derived excitatory amino acids on glutamate receptors. *JPET* **2005**, *314*, 1068–1078.
- Sasaki, M.; Maruyama, T.; Sakai, R.; Tachibana, K. Synthesis and biological activity of dysibaine model compound. *Tetrahedron Lett.* **1999**, *40*, 3195–3198.
- (a) Christensen, J. K.; Varming, T.; Ahring, P. K.; Jørgensen, T. D.; Nielsen, E. Ø. In vitro characterization of 5-carboxyl-2,4-di-benzamido-benzoic Acid (NS3763), a noncompetitive antagonist of GLU<sub>K5</sub> receptors. *J. Pharmacol. Exp. Ther.* **2004**, *309*, 1003–1010. (b) Valgeirsson, J.; Nielsen, E. Ø.; Peters, D.; Kristensen, A. S.; Madsen, U. Bioisosteric Modifications of 2-arylureidobenzoic acids: selective noncompetitive antagonists for the homomeric kainate receptor subtype GluR5. *J. Med. Chem.* **2004**, *47*, 6948–6957.
- (a) Jane, D. E.; Pook, P. C.-K.; Sunter, D. C.; Udvarhelyi, P. M.; Watkins, J. C. New willardiine analogs with potent stereoselective actions on mammalian spinal neurones. *Br. Pharmacol.* **1991**, *104*, 333P. (b) Patneau, D. K.; Mayer, M. L.; Jane, D. E.; Watkins, J. C. Activation and desensitization of AMPA/kainate receptors by novel derivatives of willardiine. *J. Neurosci.* **1992**, *12*, 595–606. (c) Wong, L. A.; Mayer, M. L.; Jane, D. E.; Watkins, J. C. Willardiines differentiate agonist binding sites for kainate-versus AMPA-preferring glutamate receptors in DRG and hippocampal neurones. *J. Neurosci.* **1994**, *14*, 3881–3897. (d) Jane, D. E.; Hoo, K.; Kamboj, R.; Deverill, M.; Bleakman, D.; Mandelzys, A. Synthesis of Willardiine and 6-Azawillardiine analogs: Pharmacological characterization on cloned homomeric human AMPA and kainate receptor subtypes. *J. Med. Chem.* **1997**, *40*, 3645–3650.
- (a) Dolman, N. P.; Troop, H. M.; More, J. C. A.; Alt, A. J.; Ogden, A. M.; Jones, S.; Morley, R. M.; Roberts, P. J.; Bleakman, D.; Collingridge, G. L.; Jane, D. E. Synthesis and pharmacology of willardiine derivatives acting as antagonists of kainate receptors. *J. Med. Chem.* **2005**, *48*, 7867–7881. (b) Dolman, N. P.; More, J. C.

- A.; Alt, A.; Ogden, A. M.; Troop, H. M.; Bleakman, D.; Collingridge, G. L.; Jane, D. E. Structure-activity relationship studies on N<sup>3</sup>-substituted willardiine derivatives acting as AMPA or kainate receptor antagonists. *J. Med. Chem.* **2006**, *49*, 2579–2592.
- (12) More, J. C. A.; Nistico, R.; Dolman, N. P.; Clarke, V. R. J.; Alt, A. J.; Ogden, A. M.; Buelens, F. P.; Troop, H. M.; Kelland, E. E.; Pilato, F.; Bleakman, D.; Bortolotto, Z. A.; Collingridge, G. L.; Jane, D. E. Characterisation of UBP296; a novel, potent and selective kainate receptor antagonist. *Neuropharmacology* **2004**, *47*, 46–64.
- (13) Barker, G. R. I.; Warburton, E. C.; Koder, T.; Aggleton, J. P.; Bashir, Z. I.; Auberson, Y.; Jane, D. E.; Brown, M. W. Kainate and NMDA glutamate receptor antagonism impairs recognition memory at different times. *J. Neurosci.* **2006**, *26*, 3561–3566.
- (14) (a) Nomura, H.; Yoshioka, Y.; Minami, I.; Synthesis of tetrahydro-2-furyl derivatives of 5-substituted uracils. *Chem. Pharm. Bull.* **1979**, *27*, 899–906. (b) Noell, C. W.; Cheng, C. C. Pyrimidines. XXI. 1-(Tetrahydro-2-furyl)pyrimidines (1). *J. Heterocycl. Chem.* **1968**, *5*, 25–28.
- (15) Dalpozzo, R.; De Nino, A.; Maiuolo, L.; Procopio, A.; Romeo, R.; Sindona, G. A convenient method for the synthesis of N-vinyl derivatives of nucleosides. *Synthesis* **2002**, *2*, 172–174.
- (16) Kametani, T.; Kigasawa, K.; Hiiragi, M.; Wakisaka, K.; Kusama, O.; Kawasaki, K.; Sugi, H. Studies on the synthesis of chemotherapeutics. I. Synthesis of 1-(2-tetrahydrofuryl)-5-fluorouracil [Ftorafur] (studies on the synthesis of heterocyclic compounds). *J. Heterocycl. Chem.* **1977**, *14*, 473–475.
- (17) Love, K. R.; Andrade, R. B.; Seeberger, P. H. Linear synthesis of a protected H-Type II pentasaccharide using glycosyl phosphate building blocks. *J. Org. Chem.* **2001**, *66*, 8165–8176.
- (18) (a) Arnold, L. D.; Drover, J. C. G.; Vederas, J. C. Conversion of serine beta-lactones to chiral alpha amino acids by copper-containing organolithium and organomagnesium reagents. *J. Am. Chem. Soc.* **1987**, *109*, 4649–4659. (b) Arnold, L. D.; Kalantar, T. H.; Vederas, J. C. Conversion of serine to stereochemically pure beta-substituted alpha-amino acids via beta-lactones. *J. Am. Chem. Soc.* **1985**, *107*, 7105–7109. (c) Ramer, S. E.; Moore, R. N.; Vederas, J. C. Mechanism of formation of serine beta-lactones by Mitsunobu cyclization: synthesis and use of L-serine stereospecifically labelled with deuterium at C-3. *Can. J. Chem.* **1986**, *64*, 706–713.
- (19) Charonnat, J. A.; Muchowski, J. M.; Nelson, P. H. The synthesis of four isomeric bithienothiepinones [1]. *J. Heterocycl. Chem.* **1983**, *20*, 1085–1087.
- (20) Prugh, J. D.; Huitric, A. C.; McCarthy, W. The synthesis and proton magnetic resonance spectra of some brominated furans. *J. Org. Chem.* **1964**, *29*, 1991–1994.
- (21) Mayer, M. L.; Ghosal, A.; Dolman, N. P.; Jane, D. E. Crystal structures of the kainate receptor GluR5 ligand binding core dimer complex with novel selective antagonists. *J. Neurosci.* **2006**, *26*, 2852–2861.
- (22) Campaigne, E.; White, R. L. Synthesis of unsymmetrical arylthiophenes and bithienyls via oxidative cyclisation of 1,3-butadiene-1-thiols. *J. Heterocycl. Chem.* **1988**, *25*, 367–373.
- (23) Steinkopf, W.; Hanske, W. Studien in der Thiophenreihe. XXXVII. Die Jodderivate des 3-Thiitoluns. *Justus Liebigs Ann. Chem.* **1937**, *532*, 236–249.
- (24) (a) Agrawal, S. G.; Evans, R. H. The primary afferent depolarizing action of kainate in the rat. *Br. J. Pharmacol.* **1986**, *87*, 345–355. (b) Bettler, B.; Boulter, J.; Hermans-Borgmeyer, I.; O'Shea-Greenfield, A.; Deneris, E. S.; Moll, C.; Borgmeyer, U.; Hollman, M.; Heinemann, S. Cloning of a novel glutamate receptor subunit, GluR5: expression in the central nervous system during development. *Neuron* **1990**, *5*, 583–595. (c) Wilding, T. J.; Huettner, J. E. Functional diversity and developmental changes in rat neuronal kainate receptors. *J. Physiol.* **2001**, *532.2*, 411–421. (d) Kerchner, G. A.; Wilding, T. J.; Huettner, J. E.; Zhuo, M. Kainate receptor subunits underlying presynaptic regulation of transmitter release in the dorsal horn. *J. Neurosci.* **2002**, *22*, 8010–8017.
- (25) Pook, P.; Brugger, F.; Hawkins, N. S.; Clark, K. C.; Watkins, J. C.; Evans, R. H. A comparison of the actions of agonists and antagonists at non-NMDA receptors of C fibres and motoneurons of the immature rat spinal cord in vitro. *Br. J. Pharmacol.* **1993**, *108*, 179–184.
- (26) More, J. C. A.; Troop, H. M.; Jane, D. E. The novel antagonist 3-CBW discriminates between kainate receptors expressed on neonatal rat motoneurons and those on dorsal root C-fibres. *Br. J. Pharmacol.* **2002**, *137*, 1125–1133.
- (27) Hogner, A.; Greenwood, J. R.; Liljefors, T.; Lunn, M. L.; Egebjerg, J.; Larsen, I. K.; Gouaux, E.; Kastrop, J. S. Competitive antagonism of AMPA receptors by ligands of different classes: crystal structure of ATPo bound to the GluR2 ligand-binding core, in comparison with DNQX. *J. Med. Chem.* **2003**, *46*, 214–221.
- (28) Word, J. M.; Lovell, S. C.; Richardson, J. S.; Richardson, D. C. Asparagine and glutamine: using hydrogen atom contacts in the choice of side-chain amide orientation. *J. Mol. Biol.* **1999**, *285*, 1735–1747.
- (29) Lovell, S. C.; Word, J. M.; Richardson, J. S.; Richardson, D. C. The penultimate rotamer library. *Proteins* **2000**, *40*, 389–408.
- (30) Lehtonen, J. V.; Still, D. J.; Rantanen, V. V.; Ekholm, J.; Björklund, D.; Iftikhar, Z.; Huhtala, M.; Repo, S.; Jussila, A.; Jaakkola, J.; Pentikäinen, O.; Nyrönen, T.; Salminen, T.; Gyllenberg, M.; Johnson, M. S. BODIL: a molecular modeling environment for structure-function analysis and drug design. *J. Comput.-Aided Mol. Des.* **2004**, *18*, 401–419.
- (31) Frisch, M. J.; Trucks, G. W.; Schlegel, H. B.; Scuseria, G. E.; Robb, M. A.; Cheeseman, J. R.; Montgomery, J. A., Jr.; Vreven, T.; Kudin, K. N.; Burant, J. C.; Millam, J. M.; Iyengar, S. S.; Tomasi, J.; Barone, V.; Mennucci, B.; Cossi, M.; Scalmani, G.; Rega, N.; Petersson, G. A.; Nakatsuji, H.; Hada, M.; Ehara, M.; Toyota, K.; Fukuda, R.; Hasegawa, J.; Ishida, M.; Nakajima, T.; Honda, Y.; Kitao, O.; Nakai, H.; Klene, M.; Li, X.; Knox, J. E.; Hratchian, H. P.; Cross, J. B.; Bakken, V.; Adamo, C.; Jaramillo, J.; Gomperts, R.; Stratmann, R. E.; Yazyev, O.; Austin, A. J.; Cammi, R.; Pomelli, C.; Ochterski, J. W.; Ayala, P. Y.; Morokuma, K.; Voth, G. A.; Salvador, P.; Dannenberg, J. J.; Zakrzewski, V. G.; Dapprich, S.; Daniels, A. D.; Strain, M. C.; Farkas, O.; Malick, D. K.; Rabuck, A. D.; Raghavachari, K.; Foresman, J. B.; Ortiz, J. V.; Cui, Q.; Baboul, A. G.; Clifford, S.; Cioslowski, J.; Stefanov, B. B.; Liu, G.; Liashenko, A.; Piskorz, P.; Komaromi, I.; Martin, R. L.; Fox, D. J.; Keith, T.; Al-Laham, M. A.; Peng, C. Y.; Nanayakkara, A.; Challacombe, M.; Gill, P. M. W.; Johnson, B.; Chen, W.; Wong, M. W.; Gonzalez, C.; Pople, J. A. *Gaussian 03*, revision C.02; Gaussian, Inc.: Wallingford, CT, 2004.
- (32) Jones, G.; Willett, P.; Glen, R. C. A genetic algorithm for flexible molecular overlay and pharmacophore elucidation. *J. Comput.-Aided Mol. Des.* **1995**, *9*, 532–549.
- (33) Jones, G.; Willett, P.; Glen, R. C.; Leach, A. R.; Taylor, R. Development and validation of a genetic algorithm for flexible docking. *J. Mol. Biol.* **1997**, *267*, 727–748.
- (34) Merritt, E. A.; Bacon, D. J. Raster3D: Photorealistic molecular graphics. *Methods Enzymol.* **1997**, *277*, 505–524.
- (35) Pentikäinen, U.; Settimo, L.; Johnson, M. S.; Pentikäinen, O. T. Subtype selectivity and flexibility of ionotropic glutamate receptors upon antagonist ligand binding. *Org. Biomol. Chem.* **2006**, *4*, 1058–1070.
- (36) Giller, S. A.; Zhuk, R. A.; Lidak, M. J.; Ziderman, A. A. GB Patent Specification 1,168,391, 1969.
- (37) Salimbeni, A.; Canevotti, R.; Paleari, F.; Poma, D.; Caliarri, S.; Fici, F.; Cirillo, R.; Renzetti, A. R.; Subissi, A.; Belvisi, L.; Bravi, G.; Scolastico, C.; Gichetti, A. N-3-Substituted pyrimidones as potent, orally active, AT1 selective angiotensin II receptor antagonists. *J. Med. Chem.* **1995**, *38*, 4806–4820.
- (38) Evans, R. H.; Francis, A. A.; Jones, A. W.; Smith, D. A. S.; Watkins, J. C. The effects of a series of omega-phosphonic alpha-carboxylic amino acids on electrically evoked and excitant amino acid-induced responses in isolated spinal cord preparations. *Br. J. Pharmacol.* **1982**, *75*, 65–75.
- (39) Korczak, B.; Nutt, S. L.; Fletcher, E. J.; Hoo, K. H.; Elliott, C. E.; Rampersad, V.; McWhinnie, E. A.; Kamboj, R. K. cDNA cloning and functional properties of human glutamate receptor EAA3 (GluR5) in homomeric and heteromeric configuration. *Recept. Channels* **1995**, *3*, 41–49.
- (40) Hoo, K. H.; Nutt, S. L.; Fletcher, E. J.; Elliott, C. E.; Korczak, B.; Deverill, R. M.; Rampersad, V.; Fantask, R. P.; Kamboj, R. K. Functional expression and pharmacological characterization of the human EAA4 (GluR6) glutamate receptor: a kainate selective channel subunit. *Recept. Channels* **1994**, *2*, 327–337.
- (41) Bleakman, D.; Ogden, A. M.; Ornstein, P. L.; Hoo, K. Pharmacological characterization of a GluR6 kainate receptor in cultured hippocampal neurons. *Eur. J. Pharmacol.* **1999**, *378*, 331–337.
- (42) Alt, A.; Weiss, B.; Ogden, A. M.; Knauss, J. L.; Oler, J.; Ho, K.; Large, T. H.; Bleakman, D. Pharmacological characterization of glutamatergic agonists and antagonists at recombinant human homomeric and heteromeric kainate receptors in vitro. *Neuropharmacology* **2004**, *46*, 793–806.
- (43) Cheng, Y. C.; Prusoff, W. H. Relationship between the inhibition constant (K<sub>i</sub>) and the concentration of inhibitor which causes 50 per cent inhibition (IC<sub>50</sub>) of an enzymatic reaction. *Biochem. Pharmacol.* **1973**, *22*, 3099–3108.